1992

Localization of a collagenous protein in the organic matrix of spicules from the octocoral Leptogorgia virgulata (Cnidaria: Gorgonacea)

Jeffrey L. Dupree

LOCALIZATION OF A COLLAGENOUS PROTEIN IN THE ORGANIC MATRIX OF SPICULES FROM THE OCTOCORAL LEPTOGORGIA VIRGULATA (Cnidaria: Gorgonacea)

A THESIS
SUBMITTED TO THE GRADUATE FACULTY
OF THE UNIVERSITY OF RICHMOND
IN CANDIDACY
FOR THE DEGREE OF
MASTER OF SCIENCE IN BIOLOGY

BY

JEFFREY L. DUPREE
B.S., WAKE FOREST UNIVERSITY, 1987

LOCALIZATION OF A COLLAGENOUS PROTEIN IN THE ORGANIC MATRIX OF SPICULES FROM THE OCTOCORAL LEPTOGORGIA VIRGULATA

BY

JEFFREY L. DUPREE

APPROVED:

COMMITTEE CHAIR

COMMITTEE MEMBERS

EXAMINING FACULTY:

TABLE OF CONTENTS

	Page
List of Figures	iv
Acknowledgements	ix
Abstract	xi
Preface	xiii
Introduction	1
Materials and Methods	3
Results	5
Discussion	9
Literature Cited	22
Figures	29
Appendix I	46
Appendix II	48
Appendix III	49
Vita	51

LIST OF FIGURES

Page

Figure 1. Illustration of octocoral anatomy according to Bayer ('61) 29

Figure 2. Summer sample illustrating the specificity of the primary antibody for the matrix (M). (July; L.R. White; 20,000x) 30

Figure 3. Summer sample treated with pre-immune serum reveals no labelling specificity (mature spicule- MS). (July; L.R. White; 20,000x) 30

Figure 4. March sample exhibiting reduced labelling in the spicule with the collagen (PC) concentration restricted to the periphery. EDBs of scleroblasts (Sc) reveal no labelling. (March; L.R. White; 20,000x) 31

Figure 5. Summer spicule with intense labelling. Concentrations are greatest on the periphery where matrix is densest. (August; L.R. White; 20,000x) 32

Figure 6. Immature January spicule (IS) with matrix specific labelling. The matrix is greatly reduced compared to the summer immature spicules. (January; EMBed 812; 20,000x) 32

Figure 7. Immature July spicule with heavy labelling exclusively on the matrix. (July; L.R. White; 15,000x) 32

Figure 8. Spicule revealing intermediate concentrations of 140 CP with the densest labelling at the periphery. (January; EMBed 812; 10,000x) 33

Figure 9. January scleroblast with unlabelled EDBs. (January; EMBed 812; 20,000x) 33

Figure 10. Aggregated scleroblasts with heavy EDB labelling. Note the peripherally concentrated, reduced matrix. (May; L.R. White; 7,500x) 34

Figure 11. Clustered scleroblast prior to appearance of an immature spicule, therefore early in the process of spiculization. Early stage of spicule formation yields maximal EDB activity. (May; L.R. White; 20,000x) 34

Figure 12. Solitary scleroblast with little or no labelling in EDBs. Note old scleroblast (arrow), still in the vicinity of its mature spicule, reveals no EDB labelling. (May; L.R. White; 10,000x) 35

Figure 13. July sample illustrating mature and immature spicules with labelling which was not restricted to the periphery. Note the greatly reduced EDB labelling. (July; L.R. White; 10,000x) 36

Figure 14. August specimen exhibiting an extremely high concentration of 140 CP throughout spicule. (August; L.R. White; 4,500x) 37

Figure 15. July scleroblast with maturing spicule. The presence of immature spicules indicate an advanced stage of matrix transport and therefore no EDB labelling is present. (July; L.R. White; 20,000x) 37

Figure 16. Clustered August scleroblasts without EDB gold labelling. By late summer transport of 140 CP into the scleroblasts has passed its peak. (August; L.R. White; 4,500x) 38

Figure 17. High magnification of August EDBs from aggregated scleroblasts reveal no label. (August; L.R. White; 20,000x) 38

Figure 18. Polyp derived secretory vesicles (SV) with possible excretory function. (August; L.R. White; 15,000x) 39

Figure 19. Secretory vesicles demonstrating exocytosis of 140 CP. (March; L.R. White; 10,000x) 39

Figure 20. January base sample with labelled EDBs in the scleroblasts and labelled membrane bounded structures with possible lysosomal (L) activity (January; EMBed 812; 15,000x) 40

Figure 21. June base sample with labelled mature spicule. Cellular structure connected to spicule apparently depositing crystalline fragments (CF) in order to facilitate extracellular spicular growth. (June; L.R. White; 20,000x) . . . 40

Figure 22. June sample with secondary sclerocytes displaying labelled structures (LS) which may be instrumental for extracellular spicule modeling. Note EDB labelling (small arrows). (June; L.R. White; 7,500x) 41

Figure 23. High magnification micrograph of crystalline fragment possibly involved with secondary growth. (June; L.R. White; 20,000x) . . . 41

Figure 24. Cortex of the axis (CA) from July tip sample illustrating minimal levels of cortical and EDB labelling in desmocytes (De). (July; L.R. White; 15,000x) 42

Figure 25. Label free cortex from June base revealing calcium carbonate structures (CC). (June; L.R. White; 15,000x) 42

Figure 26. Cortex of the axis with heavy labelling from January base sample. Note that the calcium carbonate structures have no label. (January; EMBed 812; 15,000x) 43

Figure 27. Interface between desmocytes and axial cortex from January base sample. Heavy labelling was present in the cortex but also note the labelled EDBs of the desmocytes (arrows). (January; EMBed 812; 10,000x) 43

Figure 28. Medulla of the axis (MA) from base sample with labelled fibrous bridge (FB) and tubules (small arrows). (January; EMBed 812; 7,500x) 44

Figure 29. July tip sample with labelled tubules interspersed among amorphous components. (July; L.R. White; 20,000x) 44

Figure 30. Average monthly salinities and temperatures for subtidal waters off Morehead City, N.C. (data supplied by Dr. Kirby-Smith) 45

ACKNOWLEDGEMENTS

I wish to express my sincere appreciation to the following people who were instrumental in the completion of this study: Dr. Kirby-Smith (Duke Marine Laboratory, Beaufort, N.C.) for supplying the average monthly salinities and temperatures for the waters of the collection site and Mrs. B. Tobias for their assistance in searching the literature and acquiring many interlibrary loans; Dr. Eugene Maurakis for the plotting and printing of Figure 30; Ms. Mary Farrell for the constant inconvenience which she endured by permitting me the use of her office and computer for the typing of this manuscript; Drs. William Woolcott, William Shanabruch and Herschell Emery for the time that they spent answering numerous questions; and Drs. William Woolcott and Hugh West for their willingness to provide the financial support that was required to complete this work.

I wish to thank the members of my committee: Drs. W. John Hayden and Gary Radice for their suggestions which substantially improved the quality of this study and their editing abilities. I also wish to thank Dr. Normitsu Watabe for: 1) the primary antibody, 2) technical advice and 3) financial support which allowed me to continue the research during the summer of 1990.

Finally I wish to thank my research advisor Dr. Roni Kingsley for allowing me the opportunity of working with her in her lab for the past one and one-half years. I sincerely

appreciate the time that she has invested in me and in this study to ensure its completion and her constant encouragement even in times of tremendous frustration.

ABSTRACT

Calcareous body inclusions are commonly found throughout the invertebrate taxa. Elaborately structured calcium carbonate spicules are the major mineralized body inclusions of the gorgonian, Leptogorgia virgulata. Spicule formation in this octocoral, as well as other calcium carbonate invertebrate structures, is apparently regulated by the intra-spicule organic matrix. Recent findings show that the insoluble fraction of the spicule organic matrix is collagenous. Collagen, although integral to calcium phosphate structures found in vertebrates is not usually associated with the formation of invertebrate calcium carbonate structures. Interestingly, collagen is present in the organic matrix during the summer but absent in winter. This suggests that there is a seasonal turnover of collagen. Antibodies (supplied by Dr.N. Watabe, University of South Carolina) were directed against the purified collagenous fractions from summer samples. Immunocytochemical techniques were subsequently employed at the electron microscope level and localization of this collagen fraction was determined in animals collected throughout the year. The location of the collagenous fraction of the organic matrix was determined from the time of the initial disappearance from spicules in winter to its reappearance during the following spring and summer. Several mechanisms addressing the fate of the collagen during the winter months

are discussed. In addition this study also produced the first evidence for extracellular spicule growth in L. virgulata.

PREFACE

Leptogorgia virgulata, commonly known as a sea whip, is in the Class Anthozoa and the Order Gorgonacea (Gosner, '71). As described by Bayer ('61) members of this order are polypoid and contain an axial skeleton usually composed of a proteinaceous matrix known as gorgonin. Their bodies are either extensively branched in a single plane, as the sea fan, or branched in all directions, as seen in L. virgulata (Hyman, '40).

The following is a summary of the anatomy of the polyps, spicule and axis of L. virgulata as described by Bayer ('61) (Fig. 1) except where otherwise noted. The polyps of L. virgulata are anchored in mesogleal matrix called coenenchyme. The coenenchyme is a thick gelatinous substance containing collagen and undifferentiated amoeboid cells. Some of these cells become cnidoblasts, which produce nematocysts, while others mature to scleroblasts, which form calcite crystals, known as spicules or ossicles. Polyps are interconnected by a network of tubes called solenia which transverse the coenenchyme and open into the gastric cavity. The gastric cavity is divided by eight septa, or mesenteries, which explains the common name of octocoral. The septa, which extend from the basal to the oral discs and join the pharynx on their inner edge, form eight sacs that empty into the tentacles. Filaments are located on the edges of the septa. They are equipped with

cnidocytes, reproductive cells, digestive enzyme secreting cells and muscle for retraction which provides protection of the oral disc. The presence of the pharynx in Anthozoans is taxonomically important since no other cnidarians have a comparable structure. Extending the length of the pharynx are ciliated siphonoglyphs directing food and water into the gastric cavity.

A typical branch of L. virgulata has a central axial rod that consists of a core, the medulla or central chord, which is surrounded by a hard cylindrically shaped cortex consisting of collagen (Leversee, '72). The axis is anchored to the soft tissue via cytoskeletal rod of the desmocytes (Tidball, '82).

The spicules of L. virgulata are inclusions of calcium carbonate in the form of calcite. They are the major mineralized structures of the animal and occur over an extended region of the animal's body. Spicule formation in L. virgulata (Kingsley et al., '90) and in other invertebrates (see Kingsley, '84 for review) with calcium carbonate structures is apparently regulated by the intra-spicule organic matrix. This organic matrix is composed of acidic proteins and carbohydrates and can be separated into water soluble and insoluble fractions (Kingsley and Watabe, '83).

The formation of spicules by scleroblasts in L. virgulata has been studied extensively by Kingsley and Watabe ('82). Spicule formation begins with the aggregation of scleroblasts in the mesoglea. Organic matrix is transported by Golgi vesicles to a spicule forming vacuole. Calcite crystal deposition then follows. Vacuole size increases while matrix incorporation and subsequent crystal growth continue, filling the vacuole. The scleroblasts then dissociate and spicule processes begin to form. Further spicule growth stretches the cell into a thin envelope. Fusion of the spicule forming vacuole and plasma membrane releases the spicule into the extracellular environment, where it may continue to grow. The scleroblast may atrophy or migrate from its spicule. By convention, intracellular spicules are termed immature, whereas extracellular spicules

are termed mature.

The tip region of the branches of L. virgulata is the most active area of cellular division, matrix synthesis and spicule formation (Kingsley and Watabe, '89). The mid branch and base regions contain the bulk of the colonies' spicules (Kingsley and Watabe, '89). Therefore the majority of the organic matrix in the spicules is contained in regions other than the tip (Kingsley and Watabe, '89). There have been limited studies on spicule formation in branch locations other than the tip. Therefore, the present study considered spicules from regions throughout the colony.

In a recent study by Kingsley et al. ('90), collagen was identified in the insoluble organic matrix of spicules isolated from whole colonies of L. virgulata collected during the summer. These samples displayed hydroxyproline, hydroxylysine, and glycine in ratios typical of collagen. This finding was significant since collagen has not conclusively been found in the matrices of other calcium carbonate structures of invertebrates, but is the major matrix component of calcium phosphate bones and teeth of vertebrates. SDS-Page of the insoluble matrix from spicules collected in the summer revealed a 140 kD collagenous protein (Watabe et al., '91). However collagen was not found in the matrix of winter spicules which suggests a seasonal turnover of the 140 kD collagenous protein (140 CP)

(Watabe et al., '91). The current research was conducted to localize 140 CP throughout the year and to determine the fate of 140 CP during the winter months.

Since L. virgulata exhibits tip extension growth and is collected from temperate waters, physiological differences may exist between tip tissues initiated in the summer and those that endured the winter. However, no study has analyzed such differences, but the extent of such environmental influences should be addressed in the future.

MATERIALS AND METHODS

Specimen Collection

Colonies of L. virgulata, approximately 30-35 cm in height, were collected manually from subtidal waters off Morehead City, North Carolina in January, March, May, June, July and August. Immediately following collection, branch tip segments of L. virgulata collected in all months except June, and mid and base regions from January and June were cut and processed for transmission electron microscopy (TEM).

Immunohistochemistry

Segments were rinsed in 0.2M Sorenson's buffer (pH 7.4). A subset of samples then were fixed in 2% glutaraldehyde buffered with 0.05M sodium cacodylate in filtered sea water, while others were treated with 0.05M sodium cacodylate buffered 2% paraform- aldehyde and 0.5% glutaraldehyde in filtered sea water (ie. review of

advantages and disadvantages of the two fixatives, see Appendix I). All samples were rinsed in 0.2M Sorenson's buffer, dehydrated in a series of ethanols and embedded in EMBed 812 (EM Sciences), via propylene oxide, or London Resin (L.R.) White. Two resins were employed because the chemical composition of EMBed 812 and L.R. White dictates differences in resolution and binding specificity (Causton, '84). (For review of resins, see Appendix II.)

Thin sections, 90 nm, were mounted on collodion and carbon coated nickel grids. The sections were treated with a 0.1% cetylpyridinium chloride solution in 2% paraformaldehyde buffered in 0.2M Sorenson's to enhance the organic matrix preservation (Watabe, personal communication). Sections were exposed to 1.0% bovine serum albumin for three minutes to reduce non-specific antibody binding. Following a 24 hour exposure to the primary antibody, the sections were incubated in a secondary antibody. Dilutions of 1:20, 1:80 and 1:120 were routinely used for both primary and secondary antibodies. Results were collected from sections which exhibited the least amount of random background binding.

The polyclonal primary antibody (supplied by Dr. N. Watabe) directed against the previously isolated 140 kD collagenous protein (Watabe et al., '91) was raised in male New Zealand white rabbits as described in Appendix III. Through the use of Western Blot Analysis the antibody

demonstrated specificity for the 140 kD protein (Watabe, et al., '91). Twenty nanometer gold conjugated goat anti-rabbit IgG was obtained from E.Y. Laboratories and used as the secondary antibody. This marker allowed visual localization of 140 CP. Controls were prepared by substituting the pre-immune serum (supplied by Dr. Watabe) for the primary antibody. L.R. White and EMBed 812 sections were stained with 8% uranyl acetate for 1 second and 10 minutes, respectively. Observations were made using a Philips TEM 201.

RESULTS

Primary Antibody Specificity

Localization of the primary antibody on the spicule matrix is clearly demonstrated in summer samples (Fig. 2). The specificity, tested by Western Blot Analysis (Watabe, et al., '91), is illustrated by comparing the matrix from summer spicules treated with primary antibody and those treated with pre-immune serum (Fig. 3).

Localization of 140 CP in Tip Regions

As scleroblast activity is greater in the tip (Kingsley and Watabe, '89), these regions were examined first. In comparing winter and summer spicules, the most prominent difference observed was in matrix density. The matrix of the mature spicules from both seasons labelled specifically; however, winter spicules contained less matrix and therefore less 140 CP than summer samples (Figs. 4 and 5). Similarly,

immature spicules from winter samples contained less matrix than immature spicules from summer months (Figs. 6 and 7).

The most dense labelling in mid winter specimens was observed at the peripheral regions of the spicules (Fig. 8). Examination of March spicules revealed little to no labelling, and the matrix that remained was restricted to the extreme periphery (Fig. 4). Electron dense bodies (EDBs) of January scleroblasts were also without label (Fig. 9). Spicules from March and May samples revealed similar labelling densities. However, differences were found in 140 CP localization between March and May in the scleroblasts. EDBs from May scleroblasts frequently labelled heavily (Figs. 10 and 11 while no labelling of March EDBs was observed (Fig. 4).

Not all EDBs from May samples labelled. Figure 10 shows a cluster of at least three May scleroblasts with a high degree of EDB labelling. In contrast, May EDBs were devoid of gold in solitary scleroblasts and in old scleroblasts which were commonly in close proximity of their mature spicules (Fig. 12).

July and August, gold label of the matrix increased dramatically. In both months label was found throughout the mature spicules and not exclusively on the periphery (Figs. 13 and 14). In contrast, by July, scleroblasts that were clustered or that contained immature spicules revealed less labelling of EDBs (Figs. 13 and 15). By August EDB

labelling was no longer apparent even in the aggregated scleroblasts (Figs. 16 and 17).

Although August specimens did not reveal EDB labelling, vesicles of the polyp displayed a high affinity for the gold tag complex (Fig. 18). Polyp vesicles also labelled, to a lesser degree, in March (Fig. 20).

Localization of 140 CP in Mid Branch and Base Regions

January spicules of mid branch and base regions revealed labelling patterns similar to those described for tip specimens. Mid regions were much less populated with scleroblasts than were tips in both January and June samples. Scleroblasts in the base were not observed in June but were observed in January samples. While January scleroblasts from the mid branch region were unlabelled as were those from the tips, base scleroblasts revealed moderate EDB labelling (Fig. 20). These scleroblasts also yielded labelling in membrane bounded structures (Fig. 20).

June spicules of the mid branch and base regions displayed high concentrations of the gold marker (Fig. 21). In the mid region the quantity of scleroblasts was reduced and they were absent in the base. However, a cell type of uncertain function was present in the proximity of the spicules (Fig. 22). These cells were also present in low numbers in the mid regions, however, they were abundant in the base. They were easily distinguished from scleroblasts by their numerous EDBs and transport vesicles, small nuclei

and less dense cytoplasm. These cells also contained structures that closely resembled immature spicules, but they were not enclosed in vacuoles and were restricted to the periphery of the cell (Fig. 23).

Localization of 140 CP in Axis

Structurally, there were no observable differences between the cortex of the axis of tip samples of January, June and July. However, in tip specimens the axis diameter was smaller, and calcium carbonate structures were not observed (Figs. 24 and 25). As Figures 25-27 illustrate, the calcium carbonate structures from the subtip regions demonstrated no affinity for the gold tag, and heavy cortical labelling was restricted to January base samples (Figs. 24-27).

Further labelling was observed in the desmocytes of base region specimens. These cells from January and June samples contained prominent EDBs which labelled specifically for 140 CP (Figs. 24 and 27).

Distinct differences were observed between January and June samples when comparing the medulla of the axis. The medulla of January samples from tip and mid branch contained few structural components, while an increase in structural diversity was observed in base samples (Fig. 28). These structures were of two distinct types: 1) a fibrous bridge spanning the diameter of the medulla and 2) small individual tubules. Both structures were labelled with the gold tag.

In the tip and mid branches of June samples various unlabelled amorphous structures were observed. Among these structures numerous labelled tubules were present (Fig. 29).

DISCUSSION

Seasonal 140 CP Turnover

The seasonal turnover of 140 CP, described by Kingsley et al. ('90) from assays of the insoluble matrix, was strongly supported through visualization via immunocytochemical localization of this protein. In general, summer spicules yielded the most dense label (Figs. 13 and 14), mid winter revealed an intermediate state (Fig. 8) and late winter and spring showed the lowest concentrations (Figs. 4 and 12). This suggests that the organic matrix is dynamic with a peak 140 CP influx into the spicules in late spring to early summer and a peak removal from spicules in late to early winter.

Kingsley and Watabe ('82) described the formation of immature spicules in the spicule forming vacuoles of the scleroblasts. Aggregating scleroblasts were observed in the early stages of spicule formation. During the aggregated stage a fibrous material is deposited into the spicule forming vacuole. This material presumably is the insoluble organic matrix which includes 140 CP. It is during this aggregation stage that labelling of EDBs is heaviest, and therefore, they may provide the means for 140 CP movement into the spicule forming vacuole. In support of this

theory, Dunkelberger and Watabe ('74) provided evidence that EDBs function as transport vesicles of organic matrix. They suggested that EDBs were precursors to "lolli-pop" shaped vesicles which transported the organic matrix to the spicule forming vacuole in the sea pansy Renilla reniformis, an animal in the same subclass as gorgonians. In coccolith formation of Hymenomonas carterae, small electron dense vesicles originating from the Golgi have been shown to carry both calcium and matrix material to the site of calcification (van der Wal, '85) This data suggests that the fibrous material deposited during spicule formation in L. virgulata may be 140 CP and may form the initial framework for the immature spicules.

This collagenous framework may act as a nucleator for spicule growth; however, collagen as a nucleator for mineralization in calcified tissue is a controversial topic. Wheeler and Sikes, '84 and Gunthorpe et al. ('90) stated that the soluble matrix will inhibit calcium carbonate crystal formation when free in solution. When this fraction is immobilized by crosslinkages with crab carapace, crystal formation is promoted (Gunthorpe et al., '90). Another theory suggests that collagen binds to EDTA-soluble protein which provides the site for calcification (Prockop and Williams, '82). Osteonectin may be such a protein since it strongly binds both hydroxyapatite and collagen (Termine et al., '81). However, Kingsley et al. ('87) demonstrated

recalcification in the apparent absence of soluble proteins. Mechanic et al. ('85) suggest that calcification is not initiated by soluble proteins but by the collagenous framework. They demonstrated that different collagen crosslinks were specific for mineralizing and nonmineralizing tissues (Mechanic et al., '85). Dihydroxylysinonorleucine (DHLNL) is a bifunctional crosslink found in Type I collagen of bovine bone (Mechanic et al., '71). The crosslinks found in the collagens of nonmineralizing tissues are typically multifunctional. Mechanic et al. ('85) suggest that the presence of such crosslinks holds the molecules at a shorter distance than the bifunctional crosslinks of mineralized tissue; thereby physically precluding the entrance of ions. According to Kingsley et al. ('90) 140 CP contains the bifunctional crosslink DHLNL which permits tissue calcification. Therefore, the molecular construction of 140 CP should exhibit the physical properties required for initiation of mineralization.

Evidence supporting the theory of 140 CP as a nucleator for spicule formation was provided by Kingsley et al. ('87). They stated that scleroblasts isolated from winter samples were significantly less viable (able to produce spicules) than spring scleroblasts. Furthermore, winter insoluble matrix was not able to recalcify, whereas matrix from spring tissue could recalcify. This ability was lost in winter

samples. These observations correspond with the absence of 140 CP in the organelles of in March and January scleroblasts. By spring, labelling revealed an increase in 140 CP which parallelled the increased viability of the scleroblasts. Since it has been shown that the insoluble matrix undergoes seasonal changes (Kingsley et al., '90), a subfraction that is absent during the winter yet present by spring may be the key to scleroblast viability. These observations imply that 140 CP could be involved in nucleation for spicule formation.

When scleroblast dissociation was observed, 140 CP localization was in the immature spicules and no longer seen in the EDBs. Since 140 CP concentration in the spicules was greater in the solitary scleroblasts as compared to the clustered scleroblasts, it was logical to assume that 140 CP localized in the EDBs had moved into the immature spicules.

An additional role for EDBs is suggested by van der Wal ('85) in coccolith formation and by Kingsley and Watabe ('85) in spicule formation. They provided evidence that EDBs were involved in calcium transport in scleroblasts. EDBs' may have several roles in the regulation of calcium influx. First, they may regulate the addition of calcium into the spicule forming vacuole. The calcium would then form carbonate crystals. Secondly, Gilula and Epstein ('76) proposed that continued uptake of calcium may trigger the uncoupling of aggregated scleroblasts which may be necessary

for further spicule growth. Thirdly, and perhaps most importantly, the EDBs may provide a location for the initial exposure of calcium to 140 CP. It is possible that 140 CP is imposing some initial control over the process of crystal deposition and orientation. Such control by the organic matrix is not a novel phenomena. The small electron dense vesicles in Hymenomonas carterae which contain both calcium and matrix have been described as the site for possible crystal nucleation (van der Wal, '85), and in the gorgonian Pseudoplexaura flagellosa, Goldberg and Benayahu ('87) showed that primary crystal formation occurred in Golgi derived vesicles which may contain a fibrous component of the organic matrix.

If calcification in L. virgulata and H. carterae is initiated in electron dense bodies and not in the vacuoles containing spicules or coccoliths, respectively, then the site of crystal nucleation in these invertebrates parallels vertebrates. In vertebrates, cartilaginous bone calcification begins in the zone of hypertrophic cells and not in mature bone cells of osteocytes (Brighton, '84). Therefore the process of calcification in both phyla may be initiated in areas other than the calcified structures.

Although the proposed functions of EDBs may partially explain the mode of 140 CP transport into immature spicules, they do not address 140 CP addition to mature spicules. Indirect evidence for extracellular spicule growth has been

presented (Kingsley et al., '87), however, the current study provides the first direct evidence for continued spicule growth. Evidence shown in Figures 21-23 may hold an answer to how extracellular spicules grow and how 140 CP reappears in summer mature spicules. If the cells seen in Figures 21-23 have the ability to transport and deposit the insoluble matrix into mature spicules, as these figures suggest, then a major portion of the mechanism surrounding deposition of 140 CP into mature spicules will be established. Both insoluble, including 140 CP, and soluble matrix could be shuttled to mature spicules by these cells which could explain extracellular spicule growth.

Goldberg and Benayahu ('87) described extracellular spicule growth in P. flagellosa. Polymorphic calcified crystals, termed spicule primordia, were released from primary sclerocytes. Specialized cells, called secondary sclerocytes, then used pseudopodia to orient and promote fusion of the extracellular spicule primordia into mature spicules. As described by Shimizu and Yamada ('80), larval spicule formation in the sea urchin Strongylcentrotus intermedius undergoes extracellular growth that resembles P. flagellosa. P. flagellosa (Goldberg and Benayahu, '87) and S. intermedius (Shimizu and Yamada, '80) differs from L. virgulata (Kingsley and Watabe, '82) with respect to the sequence of spicule maturation and extracellular growth, but all three organisms appear to have specialized cells for

extracellular spicule growth. Since these cells have been previously termed secondary sclerocytes in other organisms, the cell in Figure 22 will be termed accordingly. These cells may have dual functions involved with extracellular spicule growth and modelling, but currently little is understood about these processes. Work is in progress to elucidate the functions of these cells.

Kingsley and Watabe ('89) stated that the formation of immature spicules in regions other than the tip was rare. Their statement is supported by the reduction of scleroblasts in mid region and their absence in the base region of June samples. The presence of the secondary sclerocytes suggests that these regions functions as areas of extracellular spicule growth. Interestingly Kingsley and Watabe ('89) showed that calcium uptake in spicules was high at the tip, moderate at the mid branch and again high at the base. This high basal uptake of calcium may correspond to the activities of the secondary sclerocytes which may direct extracellular spicule growth. Although calcium uptake was reduced in the mid regions, it was not completely negated, and lower levels of calcium uptake should be typical of areas with fewer scleroblasts and secondary sclerocytes.

Although regulation of the seasonal turnover of spicular 140 CP is unclear, possible mechanisms will be discussed. Changes in the salinity of the ambient sea water may trigger changes in the rate of 140 CP synthesis. In an

in vitro study on the mollusc *Potamopyrgus*, Meenakshi *et al.* ('69) reported that salinity affects amino acid synthesis. As the salinity increased, amino acid synthesis in the periostracum varied. The production of some amino acids, such as lysine, histidine, glutamine and proline, increased while others, such as glycine and aspartic acid, decreased. While their study does not specifically address collagen, it does imply a direct relationship between amino acid synthesis and salinity. Two studies showed that uptake of extracellular amino acids increased with an increase in salinity (Benson-Rodenbough and Ellington, '82; Pierce and Minasian, '74), and Kasschua *et al.* ('84) demonstrated a direct link between increased salinities and an increased amino acid concentration in the sea anemone, *Bunodosoma cavernata*.

Figure 30, which charts the average monthly salinity levels for 1990 as collected by Dr. Kirby-Smith of Duke University Marine Laboratory, illustrates that the changes in the salinity parallelled the collagen turnover in *L. virgulata*. The lowest salinity was recorded in March which corresponded with minimal 140 CP concentrations in the scleroblasts and spicules. Both salinity and 140 CP increased until August when salinity began a decline and evidence for 140 CP turnover begins to emerge.

Temperature may indirectly initiate changes in the amino acid composition of the organic matrix. Calcium ion

uptake is known to increase at higher temperatures in molluscan larvae (Maeda-Martinez, '87) and in the coral Pocillopora damicornis (Clausen, '71). With the intricate association between calcium and matrix deposition in the spicule, a calcium influx triggered by rising temperatures may initiate the synthesis of the 140 CP. The data for the average monthly temperatures, presented in Figure 30, compared with the 140 CP concentrations, suggests a correlation between temperature and calcification in L. virgulata.

The decrease in spicular 140 CP in the winter indicates that this protein is in some way degraded or translocated. The labelled membrane bounded structures observed in January base scleroblasts (Fig. 20) may indicate degraded 140 CP being digested by lysosomal activity. These structures resemble membrane bounded inclusions found in the sea urchin Actinia fragacea which Larkman ('84) described as having lysosomal origin. In L. virgulata Kingsley and Watabe ('82) used histochemical techniques to localize acid phosphatase in membrane bounded inclusions in scleroblasts. However to conclude that these structures are digesting degraded 140 CP would be premature and therefore, the role of lysosomal activity and other enzymes (ie. collagenase) is currently under investigation.

Figure 18 illustrates that polyps of August specimens contain membrane bounded vesicles with a high affinity for

the gold marker. Vesicles of similar size and density have been described in epidermal gland cells of the flatworm Didymorchis (Rohde and Watson, '90) and in ectodermal mucous cells of the sea pen Ptilosarcus guerneyi (Crawford and Chia, '74) and were attributed the function of transport. Assuming these vesicles are involved in transport, it is uncertain whether 140 CP is entering (endocytosis) or leaving (exocytosis) the cells. It is unlikely that their vesicles are demonstrating endocytosis of 140 CP because in late summer, spicule formation is declining and the accompanying need for 140 CP should decline as well. The greatest demand for 140 CP seems to exist in late spring when formation of immature spicules is highest, it is therefore likely that labelled transport vesicles in August are beginning the turnover process. That is, 140 CP is being exocytosed from the cells via these vesicles.

The heavy labelling of these excretion vesicles may suggest the initial sign of 140 CP turnover. High levels of 140 CP excretion through the polyp of L. virgulata could continue through late winter when levels of spicular 140 CP are substantially lower. Vesicles from March specimens revealed a slight affinity for the 140 CP antibody (Fig. 19). This low level 140 CP excretion suggests a reduced but continued efflux of the protein until late spring. Presumably this excretion stops in late spring and early summer when new spicule formation occurs. Exocytosis then

resumes in the late summer. This mechanism begins to explain the fate of 140 CP.

While removal of 140 CP from the organism is possible, it could also be merely removed from the spicules and stored elsewhere in the animal during winter. Heavy labelling of the January base cortex suggests that the large base may store 140 CP. This 140 CP storage may play several roles. First, additional collagen in the axis may enable the colony to remain perpendicular to the current in more turbulent winter waters. Orientation with respect to current has been shown to play an important role in feeding (Leversee, '76). Secondly, the storage of 140 CP could conserve energy assuming that transport and storage is more energy efficient than decomposition and synthesis. Thirdly, the organism may store many compounds essential for growth and survival in the base. With the increased stress caused by the winter months, the base may provide a safe harbor. Tips regenerate easily (Kingsley et al., '87) and are the fastest calcifying area of coral colonies (Goreau, '59). Therefore the loss of the tip during the winter months may be a common occurrence, and has been observed (Kingsley, unpublished). By storing proteins in the base, loss of essential macromolecules via tip shedding is minimized. This reasoning is also supported by the continued EDB activity of the scleroblasts of January base samples. The presence of light EDB labelling suggests that a low level of scleroblast activity continued through

January in the base regions.

Some means of transport is needed to move the stored 140 CP from the axis to the mature spicules and scleroblasts. The numerous labelled tubules observed in the June and January axes (Figs. 28 and 29) are a potential transport system. These tubules may be involved in 140 CP transport both up and down the colony depending on the season. EDBs of the desmocytes may also play a role in 140 CP transport (Figs. 24 and 27). When the 140 CP reaches the appropriate level via the tubules, the EDBs may shuttle the 140 CP from the axis to the spicules. Labelled EDBs were observed in both summer and winter; therefore, they may carry the 140 CP in and out of the axis. Movement of 140 CP should be prominent in both January and June samples. January spicules are in an intermediate state of 140 CP concentration and therefore should still be shuttling 140 CP into winter storage. Since the initial signs of 140 CP turnover are not observed until August, June specimens should still be moving 140 CP up the axis presumably by these tubules. (Fig. 29)

In summary, 140 CP may be transported into immature spicules by EDBs beginning in the spring. The protein appears to reach maximal levels in spicules by mid to late summer. At this time the seasonal turnover, as described by Kingsley et al. ('90), begins. Turnover of spicular 140 CP may depend upon: 1) winter storage in base cortex

transported by axial tubules and EDBs of desmocytes, 2) excretion with or without enzymatic degradation and 3) changes in the rate of 140 CP synthesis which may be dependent upon environmental conditions.

LITERATURE CITED

Bayer, F.M. (1961) The shallow-water Octocorallia of the West Indian region. Martinus Nijhoff, The Hague.

Benson-Rodenbough, B. and W.R. Ellington. (1982) Responses of the euryhaline sea anemone, Bunodosoma cavernata (BOSC) (Antozoa, Actinaria, Actiniidae) to osmotic stress. Comp. Biochem. Physiol. 72A: 731-735.

Brighton, C.T. (1984) The growth plate. Orthopedic Clinics of North America. 15(4):571-595.

Causton, B.E. (1984) The choice of resins for electron immunocytochemistry. Pp 29-36. In: Immunolabelling for electron microscopy: J.M. Polak and I.M. Varndell, eds. Elsevier Science Publishers B.V., London.

Clausen, C. (1971) Effects of temperature on the rate of ^{45}calcium uptake by Pocillopora damicornis. Pp 246-259. In: Experimental Coelenterate Biology, eds. H.M. Lenhoff, L. Muscatine L.V. Davis. University of Hawaii Press, Honolulu.

Crawford, B.J. and F-S. Chia. (1974) Fine structure of the mucous cell in the sea pen, Ptilosarcus guerneyi, with special emphasis on the possible role of microfilaments in the control of mucus release. Canadian Journal of Zoology 52: 1427-1432.

Dunkelberger, D.G. and N. Watabe. (1974) An ultrastructural study on spicule formation in the Pennatulid colony Renilla reniformis. Tissue Cell Res. 6: 573-586.

Gilula, N.B. and M.L. Epstein. (1976) Cell-to-cell communication, gap junctions and calcium. Pp 257-272. In: Calcium in biological systems. Symposia of the Society of Experimental Biology No. 30. Cambridge University Press, Cambridge England.

Goldberg, W.M. and Y. Benayahu. (1987) Spicule formation in the gorgonian coral Pseudoplexaura flagellosa. I: Demonstration of intracellular and extracellular growth and the effect of ruthenium red during decalcification. Bulletin of Marine Science 40(2): 287-303.

Goreau, T.F. (1959) The physiology of skeleton formation in corals. I. A method for measuring the rate of calcium deposition by corals under different conditions. Biological Bulletin, Woods Hole 116: 59-75.

Gosner, K.L. (1971) Guide to identification of marine and estuarine invertebrates: Cape Hatteras to the Bay of Fundy. Pp. 143-145. Wiley-Interscience, Inc. New York.

Gunthorpe, M.E., C.S. Sikes and A.P. Wheeler. (1990) Promotion and inhibition of calcium carbonate crystallization in vitro by matrix protein from the blue crab exoskeleton. Biol. Bull. 179: 191-200.

Hayat, M.A. (1981) Principles and techniques of electron microscopy biological applications, Volume 1, 2nd edition. University Park Press, Baltimore, pp 34-68.

Hyman, L.M. (1940) The invertebrates. Vol.I. Protozoa through ctenophore. McGraw-Hill, New York.

Kasschau, M.R., J.B. Ragland, S.O. Pinkerton, and E.C.M. Chen. (1984) Time related changes in the free amino acid pool of the sea anemone, Bunodosoma cavernata, during salinity stress. Comp. Biochem. Physiol. 79A: 155-159.

Kingsley, R.J. and N. Watabe. (1982) Ultrastructural investigation of spicule formation in the gorgonian Leptogorgia virgulata (Lamarck) (Coelenterata: Gorgonacea). Cell Tissue Res. 223: 325-334.

Kingsley, R.J. and N. Watabe. (1983) Analysis of proteinaceous components of the organic matrixes of spicules from the gorgonian Leptogorgia virgulata. Comp. Biochem. Physiol. 76B: 443-447.

Kingsley, R.J. (1984) Spicule formation in the invertebrates with special reference to the gorgonian Leptogorgia virgulata. Amer. Zool. 24:883-891.

Kingsley, R.J. and N. Watabe. (1985) Synthesis and transport of the organic matrix of the spicules in the gorgonian Leptogorgia virgulata (Lamarck). Cell Tissue Res. 235: 533-538.

Kingsley, R.J., M. Bernhardt, K. Wilbur and N. Watabe. (1987) Scleroblast cultures from the gorgonian Leptogorgia virgulata (Lamarck) (Coelenterata: Gorgonacea). In Vitro Cellular and Developmental Biology 23(4): 297-302.

Kingsley, R.J. and N. Watabe. (1989) The dynamics of spicules calcification in whole colonies of the gorgonian Leptogorgia virgulata (Lamarck) (Coelenterata: Gorgonacea). J. Exp. Mar. Biol. Ecol. 133: 57-65.

Kingsley, R.J., M. Tsuzaki, N. Watabe and G.L Mechanic. (1990) Collagen in the spicule organic matrix of the gorgonian Leptogorgia virgulata. Biological Bulletin 179: 207-213.

Laemmli, U.K. and M. Favre. (1973) Maturation of the head of bacteriophage T4I. DNA packing events. Journal of Molecular Biology 80: 575-599.

Larkman, A.U. (1984) The fine structure of granular amoebocytes from the gonads of the sea anemone Actinia fragacea (Cnidaria: Anthozoa). Protoplasma 122: 203-221.

Leversee, G.L. (1972) Organization and synthesis of the axial skeleton of Leptogorgia virgulata. Ph.D. Thesis, Duke University, Durham, N.C. 1-130.

Leversee, G.J. (1976) Flow and feeding in fan-shaped colonies of the gorgonian coral, Leptogorgia. Biol. Bull. 151: 344-356.

Maeda-Martinez, A.N. 1987. The rates of calcium deposition in shells of molluscan larvae. Comp. Biochem. Physiol. 86A: 21-28.

Mechanic, G.L., M. Gallop and M.L. Tanzer. (1971) The nature of crosslinking in collagens from mineralized tissues. Biochem. Biophys. Res. Comm. 45: 644-653

Mechanic, G.L., A.J. Banes, M. Henmi and M. Yamauchi. (1985) Possible collagen structural control of mineralization. Pp. 98-108. In: The chemistry and biology of mineralized tissues. W.T. Butler, ed. EBSCO Media, Birmingham.

Meenakshi, V.R., P.E. Hare, N. Watabe and K.M. Wilbur. (1969) The chemical composition of the periostracum of the molluscan shell. Comp. Biochem. Physiol. 29A: 611-620.

Pierce, Jr.,S.K. and L.L. Minasian, Jr. (1974) Water balance of a euryhaline sea anemone, Diadumene leucolena. Comp. Biochem. Physiol. 49A: 159-167.

Prockop, D.J. and C.J. Williams. (1982) Structure of the organic matrix: collagen structure (chemical). Pp. 161-177. In: Biological mineralization and demineralization. G.H. Nancollae, ed. Springer-Verlag, New York.

Rohde, K. and N. Watson. (1990) Epidermal and subepidermal structures in Didymorchis (Platyhelminthes, Rhabdocoela).II. Ultrastructure of gland cells and ducts. Zool. Anz. 224: 276-285.

Roth, J. (1984) The protein A-gold technique for antigen localization in tissue sections by light and electron microscopy. Pp 113-120. In: Immunmolabelling for electron microscopy: J.M. Polak and I.M. Varndell, eds. Elsevier Science Publishers B.V., London.

Shimizu, M. and J. Yamada. (1980) Sclerocytes and crystal growth in the regeneration of sea urchin test and spines. Pp. 168-178. In: The mechanism of biomineralization in animals and plants. M. Omori and N. Watabe, eds. Tokai University Press, Tokyo.

Termine, J.D., H.K. Kleinman, S.W. Whitson, H.M. Conn, M.L. McGarvey and G.R. Martin. (1981) Osteonectin, a bone-specific protein linking mineral to collagen. Cell

Tidball, J.G. (1982) Fine structural aspects of Anthozoan desmocyte development (Phylum Cnidaria). Tissue and Cell 14(1): 85-96.

van der Wal, P., W. C. de Bruijn and P. Westbroek. (1985) Cytochemical and x-ray microanalysis studies of intracellular calcium pools in scale bearing cells of the coccolithophorid Emiliania huxleyi. Protoplasma 124:1-9.

Watabe, N., M. Oishi and R.J. Kingsley. (1991) The organic matrix spicules of the gorgonian Leptogorgia virgulata. Pp 9-16. In Mechanisms and Phylogeny of Mineralization in Biological Systems, S. Suga and H. Nakahara, eds. Springer-Verlag, Tokyo.

Wheeler, A.P. and C.S. Sikes. (1984) Regulation of carbonate calcification by organic matrix. Am. Zool. 24: 933-944.

Figure 1. Illustration of octocoral anatomy according to Bayer ('61).

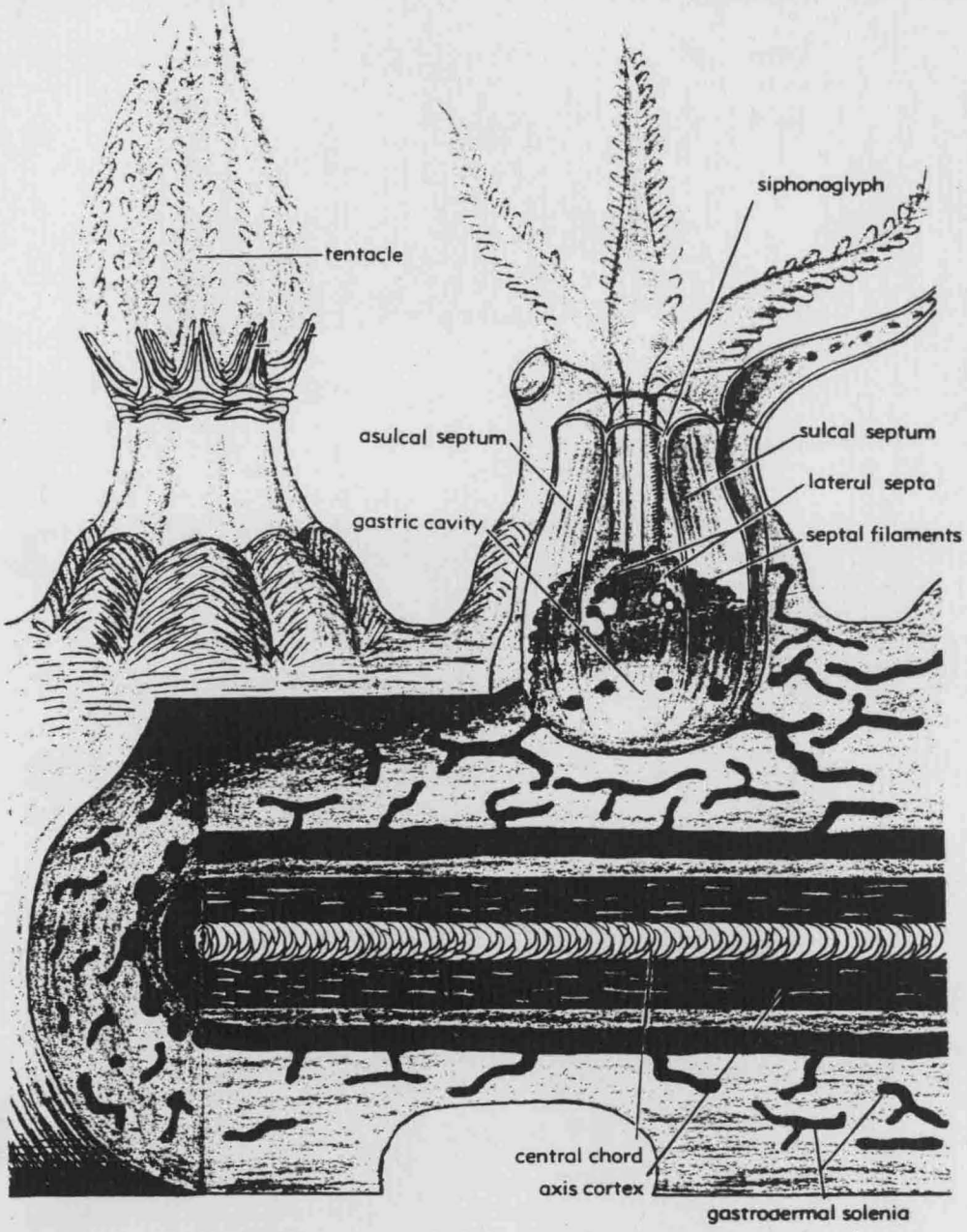
siphonoglyph
tentacle
asulcal septum
sulcal septum
lateral septa
gastric cavity
septal filaments
central chord
axis cortex
gastrodermal solenia

Figure 2. Summer sample illustrating the specificity of the primary antibody for the matrix (M). (July; L.R. White; 20,000x)

Figure 3. Summer sample treated with pre-immune serum reveals no labelling specificity (mature spicule- MS). (July; L.R. White; 20,000x)

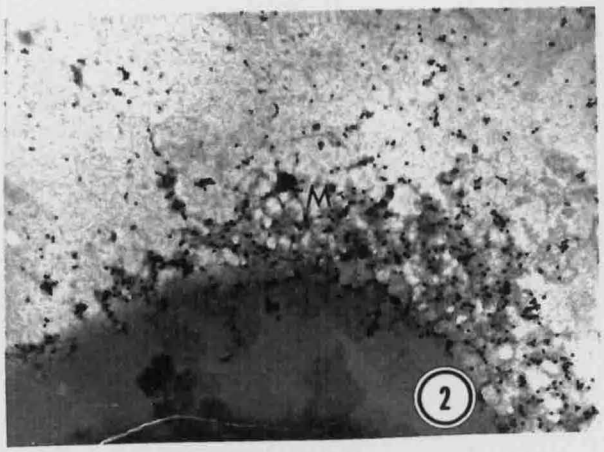
M
2

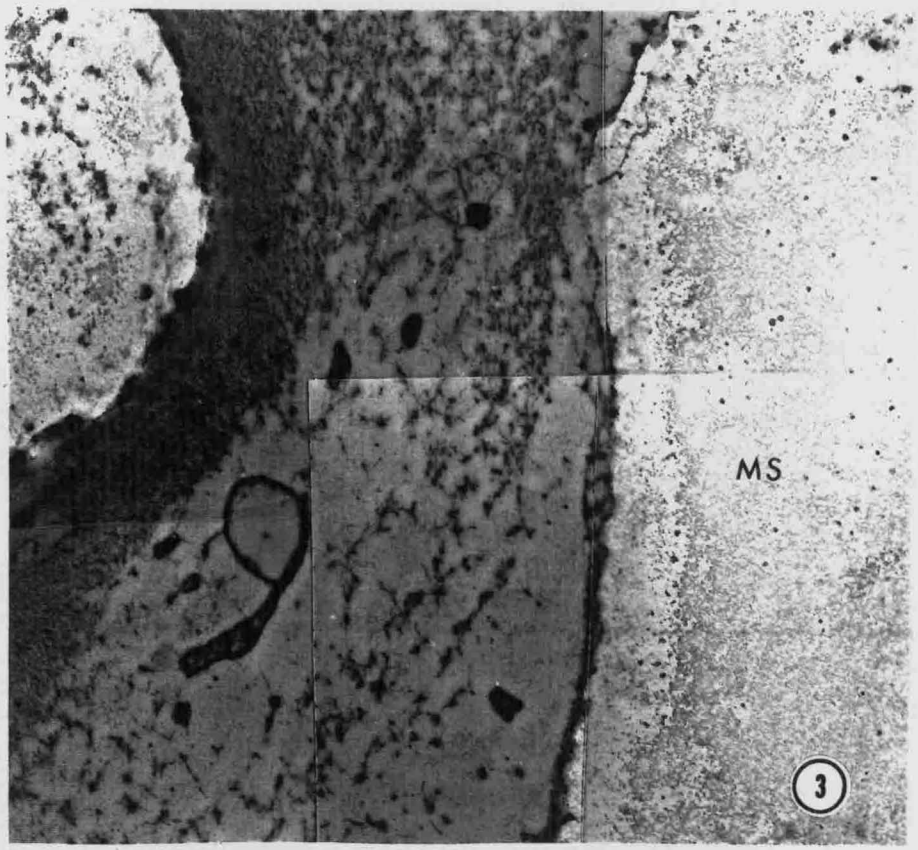
MS
3

Figure 4. March sample exhibiting reduced labelling in the spicule with the collagen (PC) concentration restricted to the periphery. EDBs of scleroblasts (Sc) reveal no labelling. (March; L.R. White; 20,000x)


EDB
EDB
PC
4

Figure 5. Summer sample with intense labelling. Concentrations are greatest on the periphery where matrix is densest. (August; L.R. White; 20,000x)

Figure 6. Immature January spicules (IS) with matrix specific labelling. The matrix is greatly reduced compared to the summer immature spicules. (January; EMBed 812; 20,000x)

Figure 7. Immature July spicule with heavy labelling exclusively on the matrix. (July; L.R. White; 15,000x)

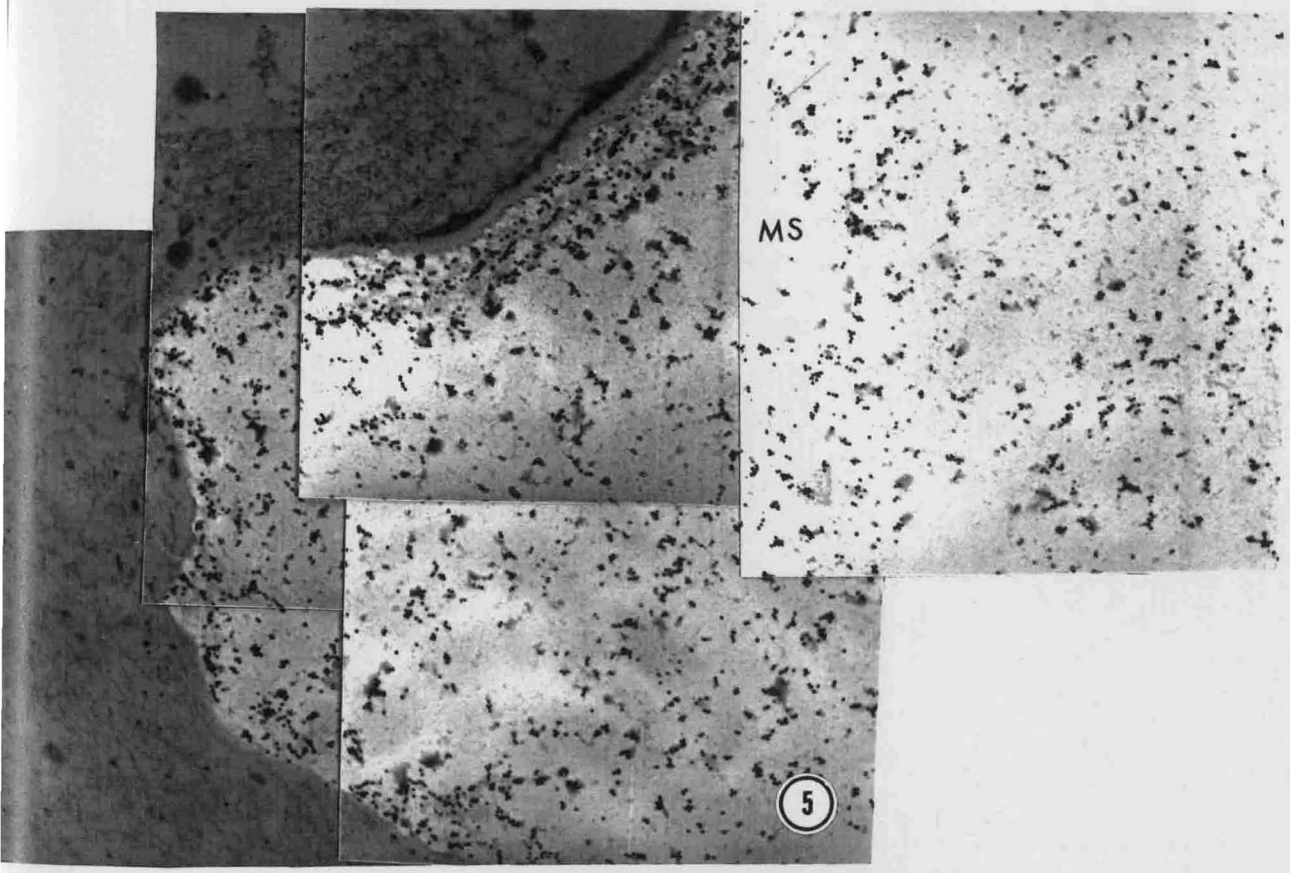
MS
5

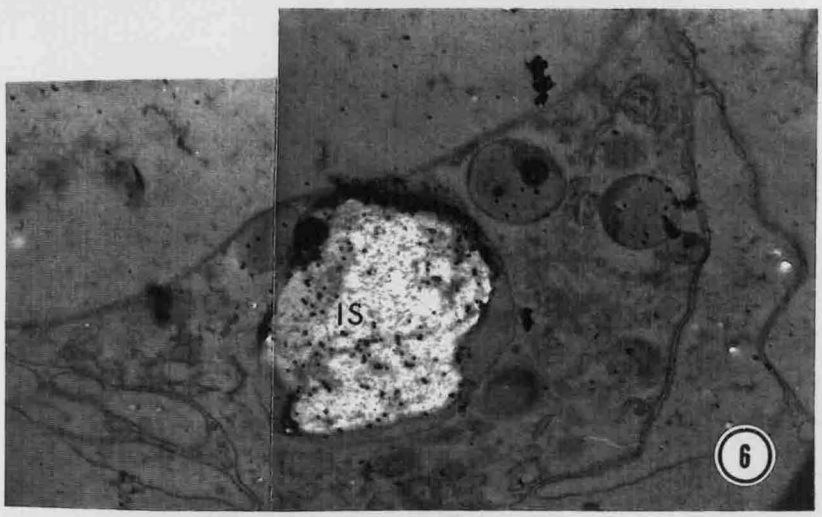
IS
6

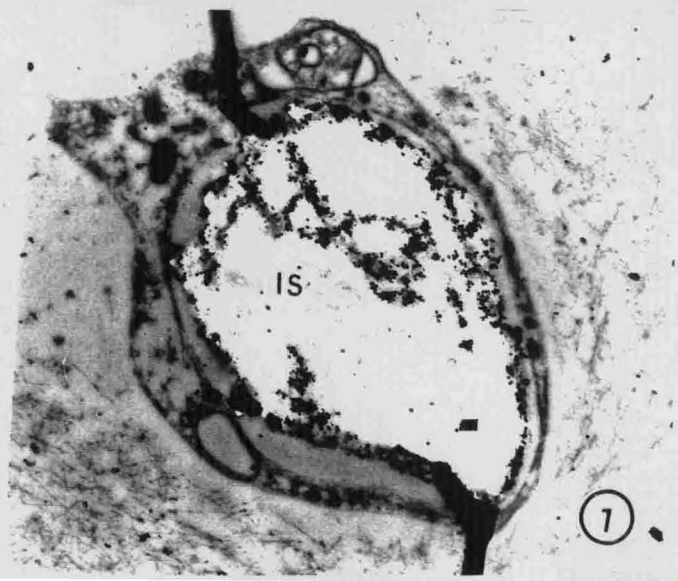
IS
7

Figure 8. Spicule revealing intermediate concentrations of 140 CP with the densest labelling at the periphery. (EMBed 812; 10,000x)

Figure 9. January scleroblast with unlabelled EDBs (January; EMBed 812; 20,000x)

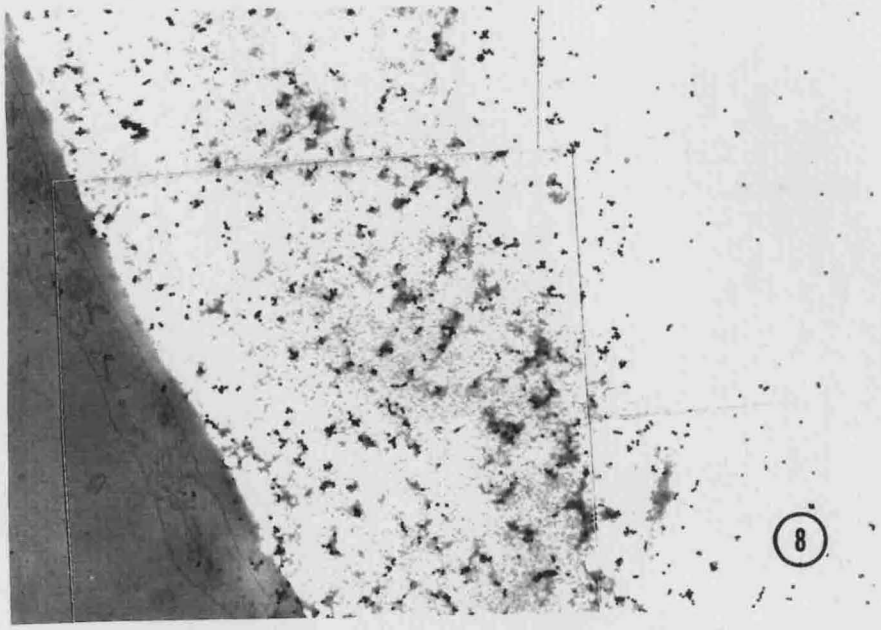
8

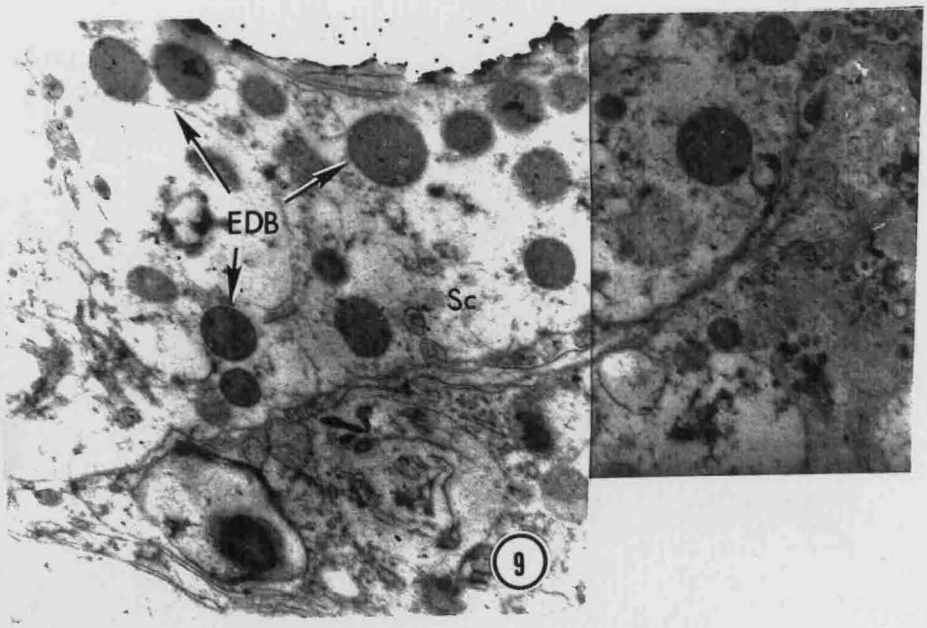
EDB
Sc
9

Figure 10. Aggregated scleroblasts with heavy EDB labelling. Note the periphery concentrated, reduced matrix. (May; L.R. White; 4,500x)

Figure 11. Clustered scleroblast prior to appearance of an immature spicule, therefore early in the process of spiculization. Early stage of spicule formation yields maximal EDB activity. (May; L.R. White; 20,000x)

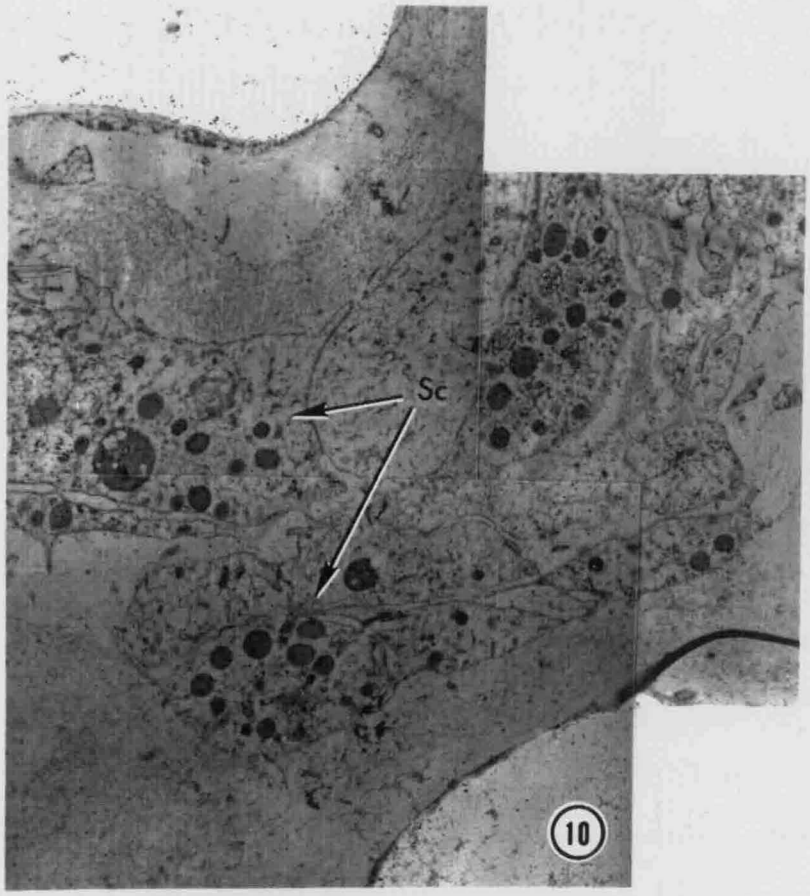
Sc
10

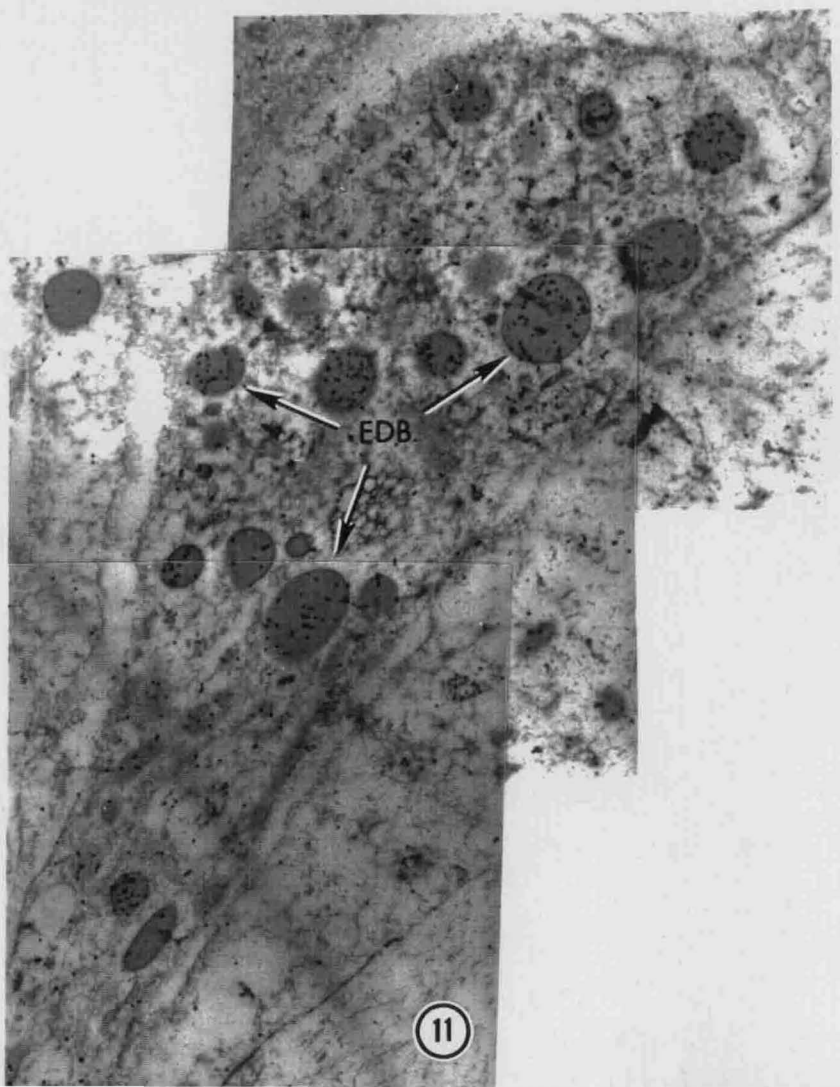
EDB
11

Figure 12. Solitary scleroblast with little or no labelling in EDBs. Note old scleroblast (arrow), still in the vicinity of its mature spicule, reveals no EDB labelling. (May; L.R. White; 10,000x)

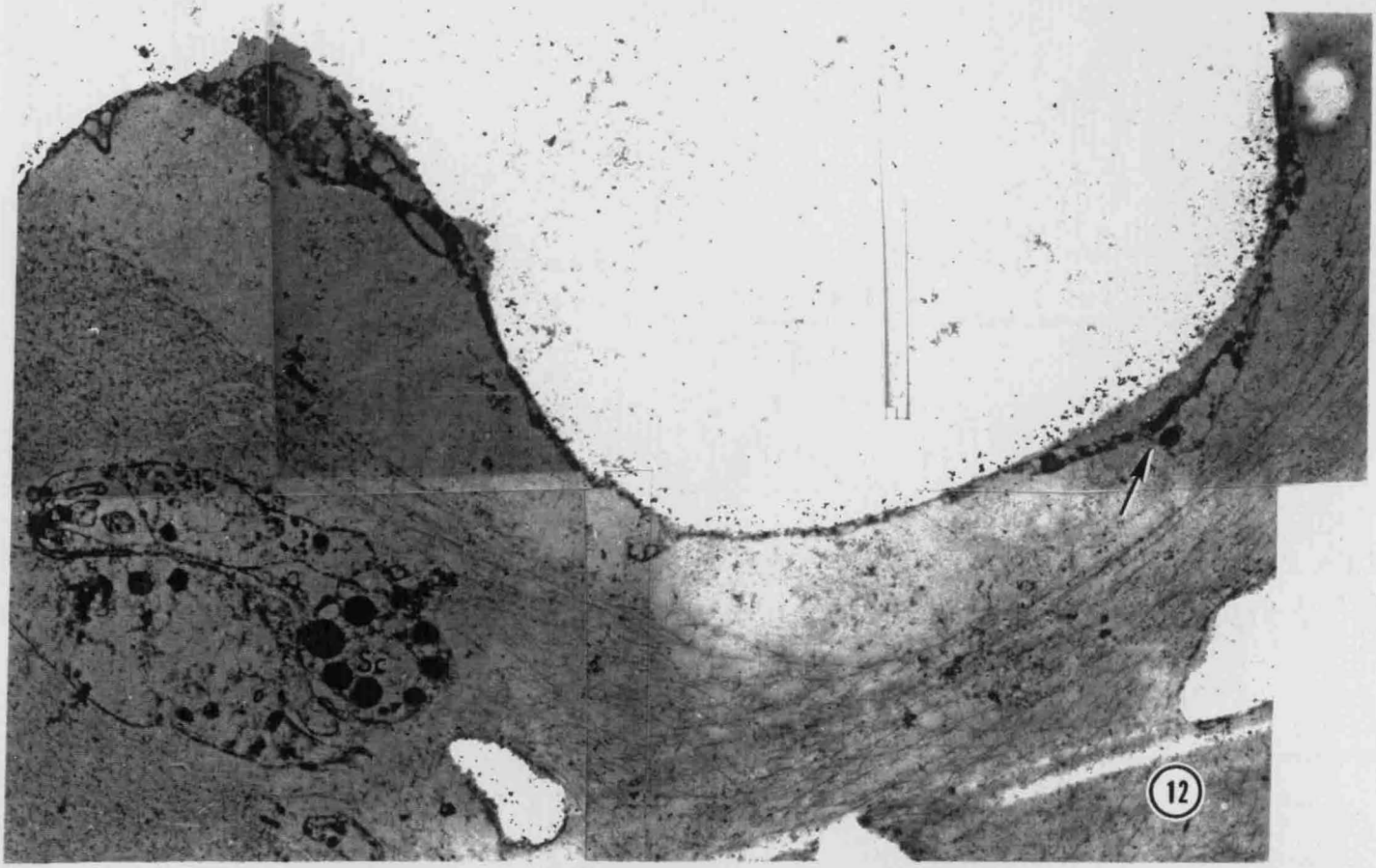
Sc
12

Figure 13. July sample illustrating mature and immature spicules. Both have intense gold labelling which was not restricted to the periphery. Note the greatly reduced EDB labelling. (July; L.R. White; 10,000x)


IS
MS
13

Figure 14. August specimen exhibiting an extremely high concentration of 140 CP throughout spicule. (August; L.R. White; 4,500x)

Figure 15. July scleroblast with maturing spicule. The presence of immature spicules indicate an advanced stage of matrix transport and therefore no EDB labelling is present. (July; L.R. White; 20,000x)

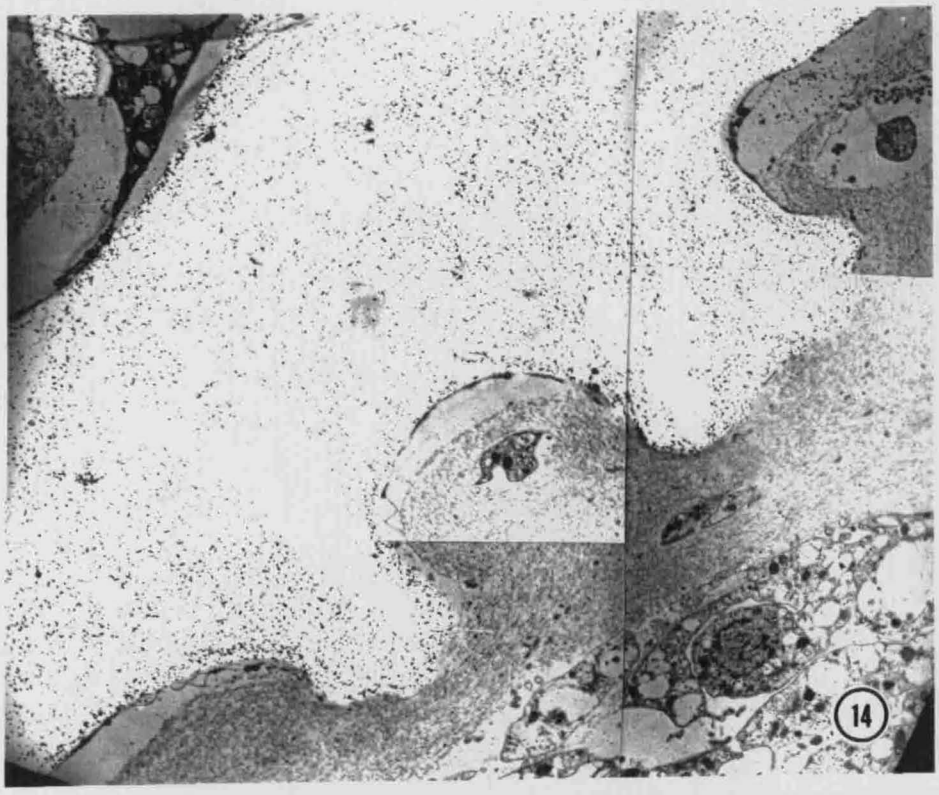
14

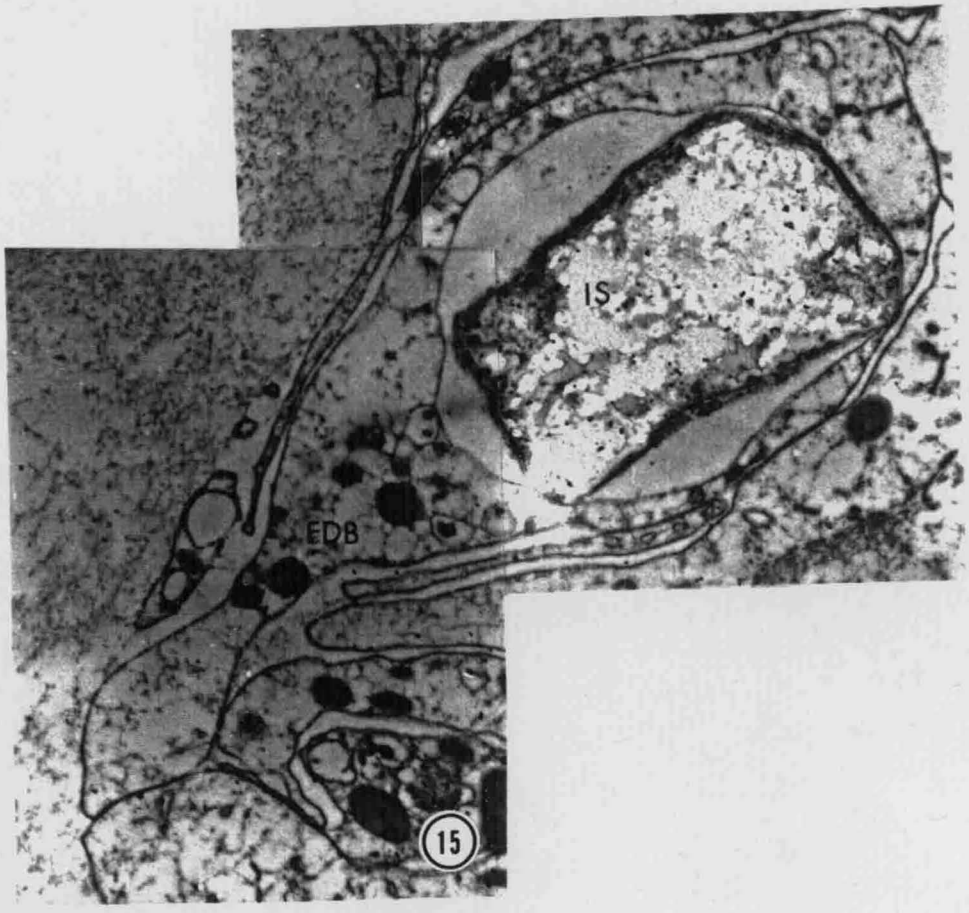
IS
EDB
15

Figure 16. Clustered August scleroblasts without EDB gold labelling. By late summer transport of 140 CP into the scleroblasts has passed its peak. (August; L.R. White; 4,500x)

Figure 17. High magnification of August EDBs from aggregated scleroblasts reveal no label. (August; L.R. White; 20,000x)

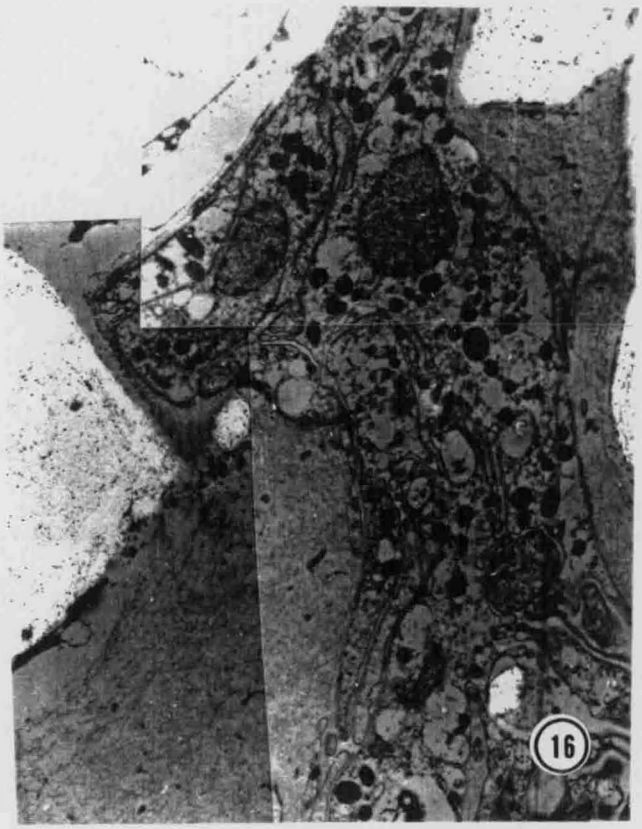
16

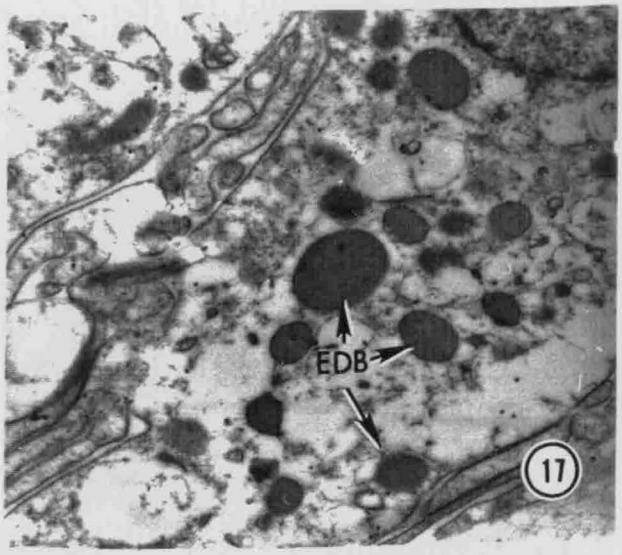
EDB
17

Figure 18. Polyp derived secretory vesicles (SV) with possible excretory function. (August; L.R. White; 15,000x)

Figure 19. Secretory vesicles demonstrating exocytosis of 140 CP. (March; L.R. White; 10,000x)

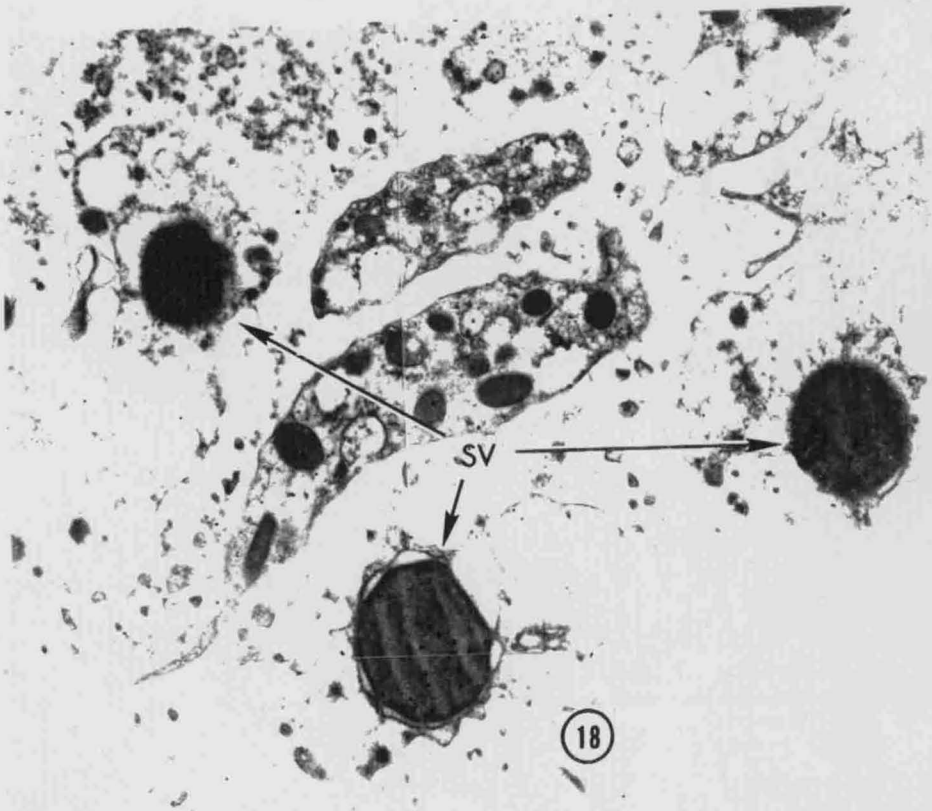
SV
18

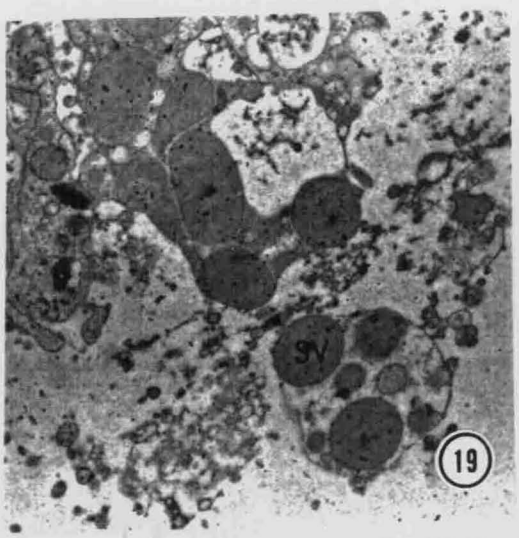
SV
19

Figure 20. January base sample with labelled EDBs in the scleroblasts and labelled membrane bounded structures with possible lysosomal (L) activity. (January; EMBed 812; 15,000x)

Figure 21. June base sample with labelled mature spicule. Cellular structure connected to spicule apparently depositing crystalline fragments (CF) in order to facilitate extracellular spicular growth. (June; L.R. White; 20,000x)

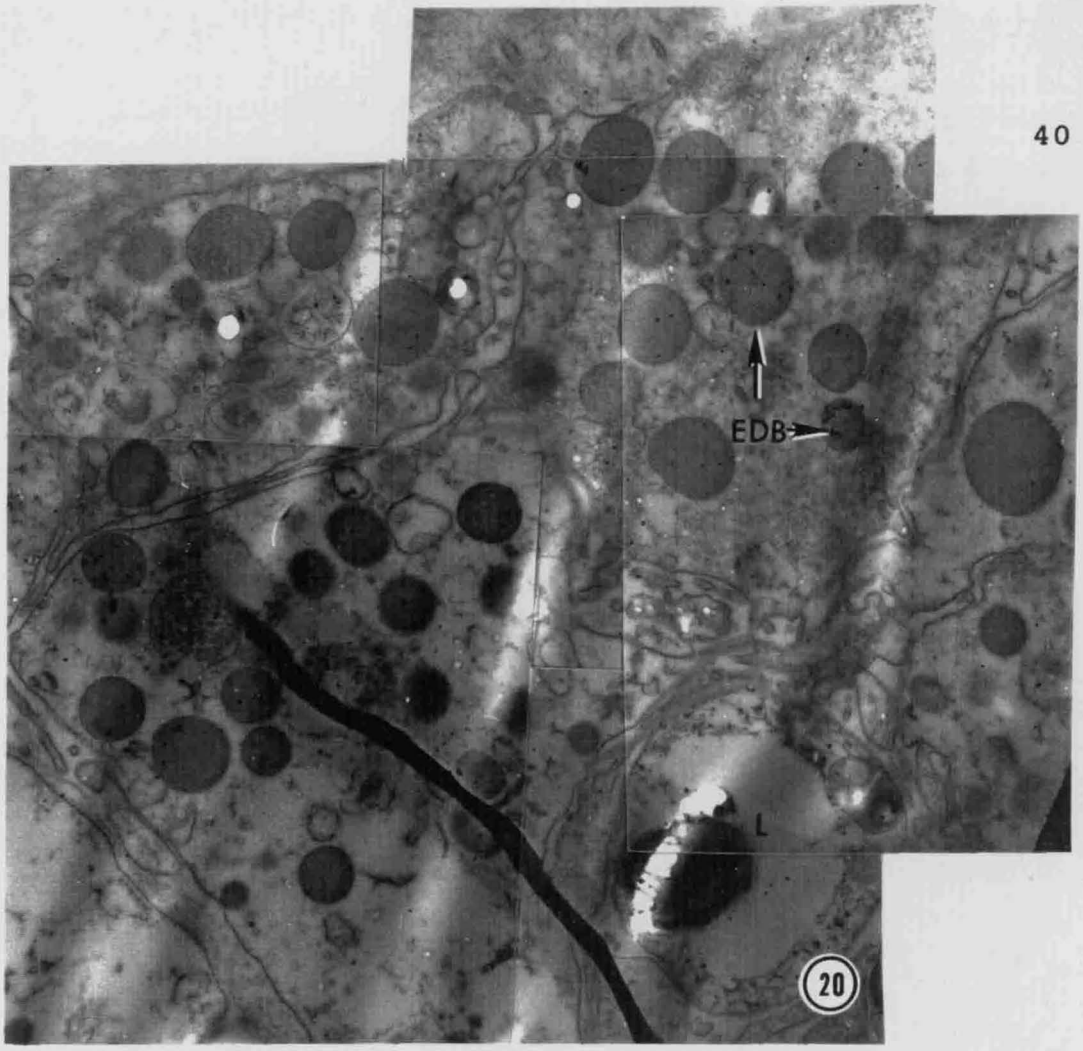
EDB
L
20

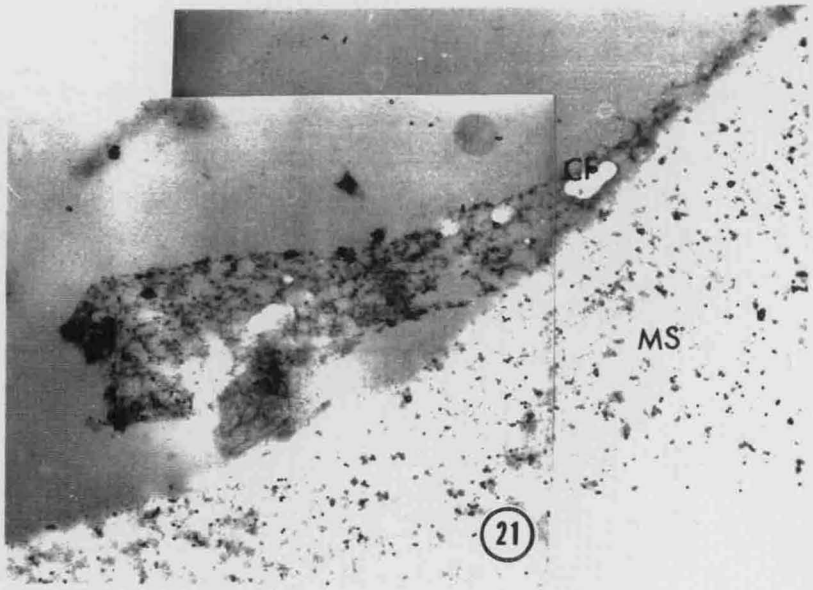
CF
MS
21

Figure 22. June sample with secondary sclerocytes displaying labelled structures (LS) which may be instrumental for extracellular spicule modeling. Note EDB labelling (small arrows). (June; L.R. White; 7,500x)

Figure 23. High magnification micrograph of crystalline fragment possibly involved with secondary growth. (June; L.R. White; 20,000x)

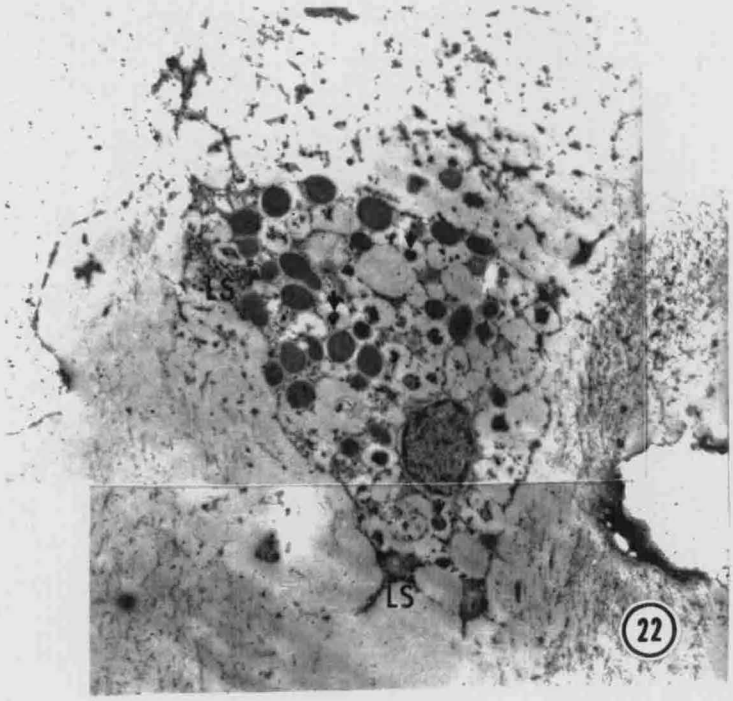
LS
LS
22

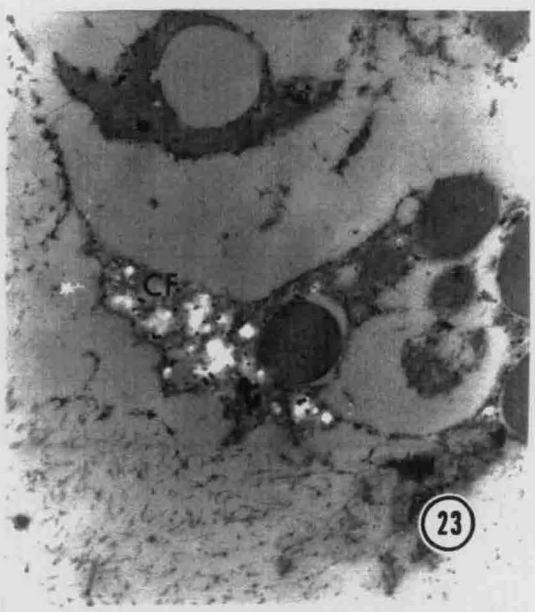
CF
23

Figure 24. Cortex of the axis (CA) from July tip sample illustrating minimal levels of cortical and EDB labelling in desmocytes (De). (July; L.R. White; 15,000x)

Figure 25. Label free cortex from June base revealing calcium carbonate srtuctures (CC). (June; L.R. White; 15,000x)

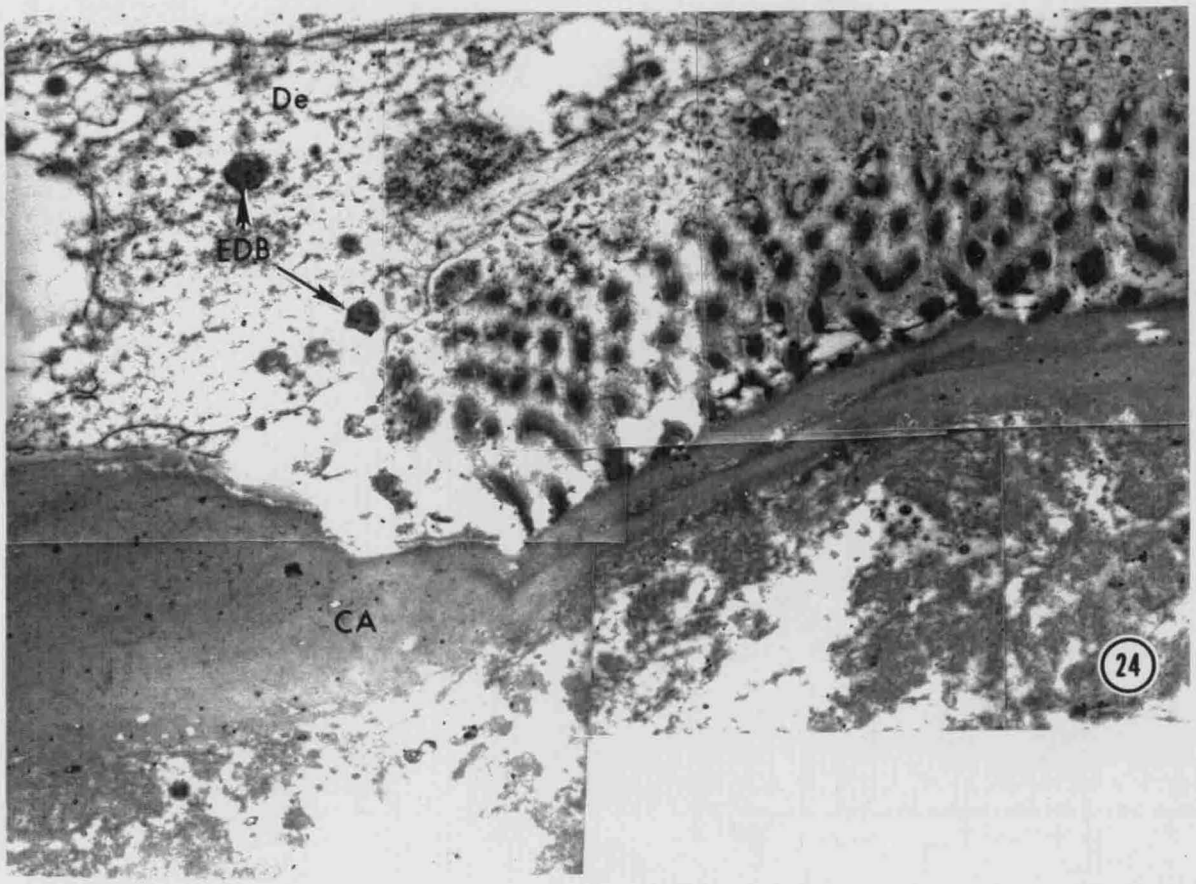
De
EDB
CA
24

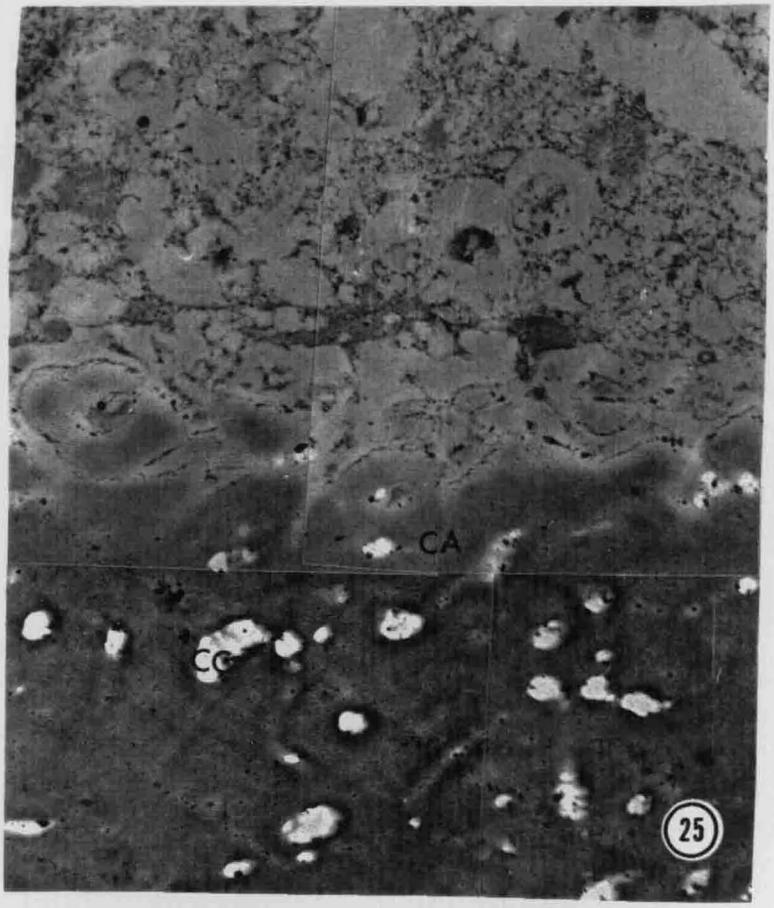
CA
CC
25

Figure 26. Cortex of the axis with heavy labelling from January base sample. Note that the calcium carbonate structures are label free. (January; EMBed 812; 15,000x)

Figure 27. Interface between desmocytes and axial cortex from January base sample. Heavy labelling was present in the cortex but also note the labelled EDBs of the desmocytes (arrows). (January; EMBed 812; 10,000x)

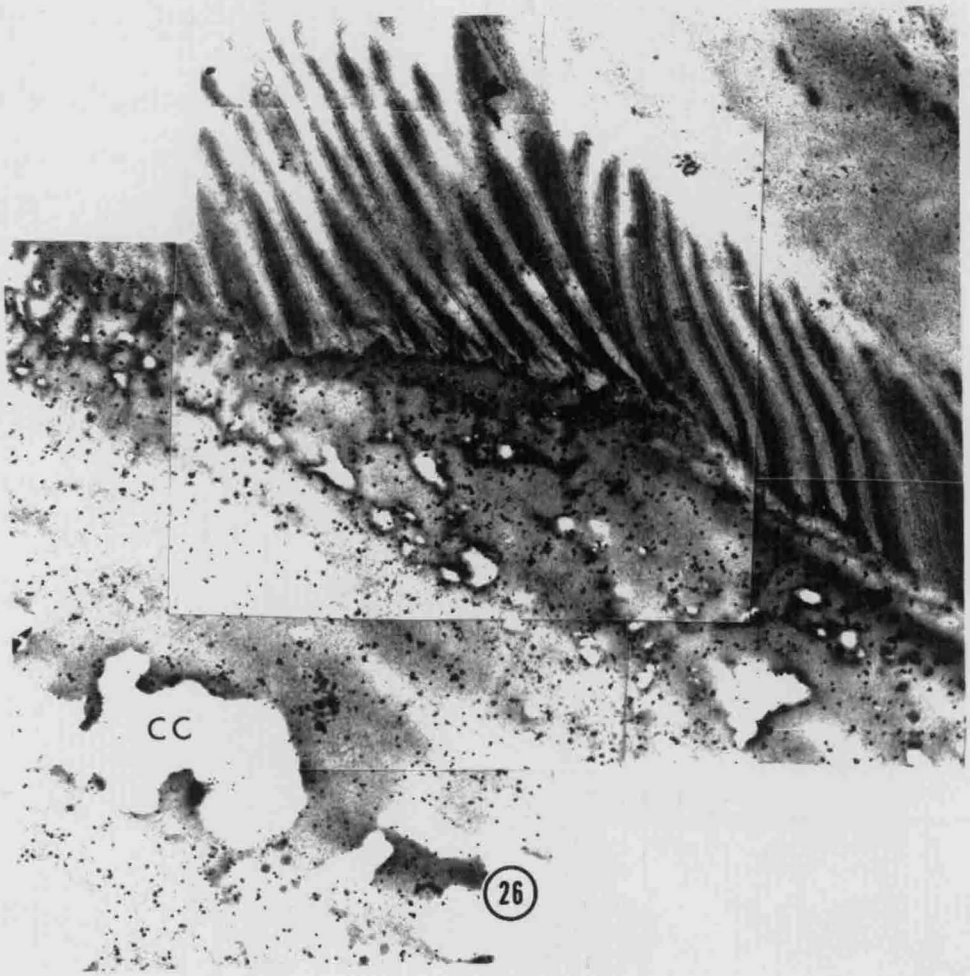
CC
26


27

Figure 28. Medulla of the axis (MA) from base sample with labelled fibrous bridge (FB) and tubules (small arrows). (January; EMBed 812; 7,500x)

Figure 29. July tip sample with labelled tubules interspersed among amorphous components. (July; L.R. White; 20,000x)

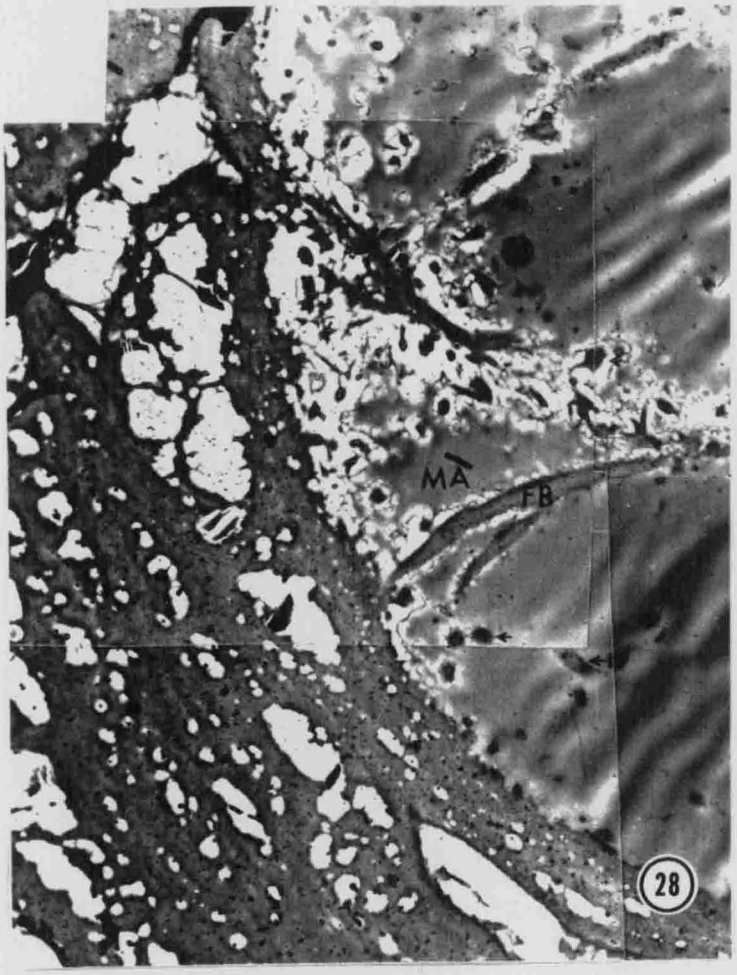
MA
FB
28


29

Figure 30. Average monthly salinities and temperatures for subtidal waters off Morehead City, N.C. (data collected by Dr. Kirby-Smith)

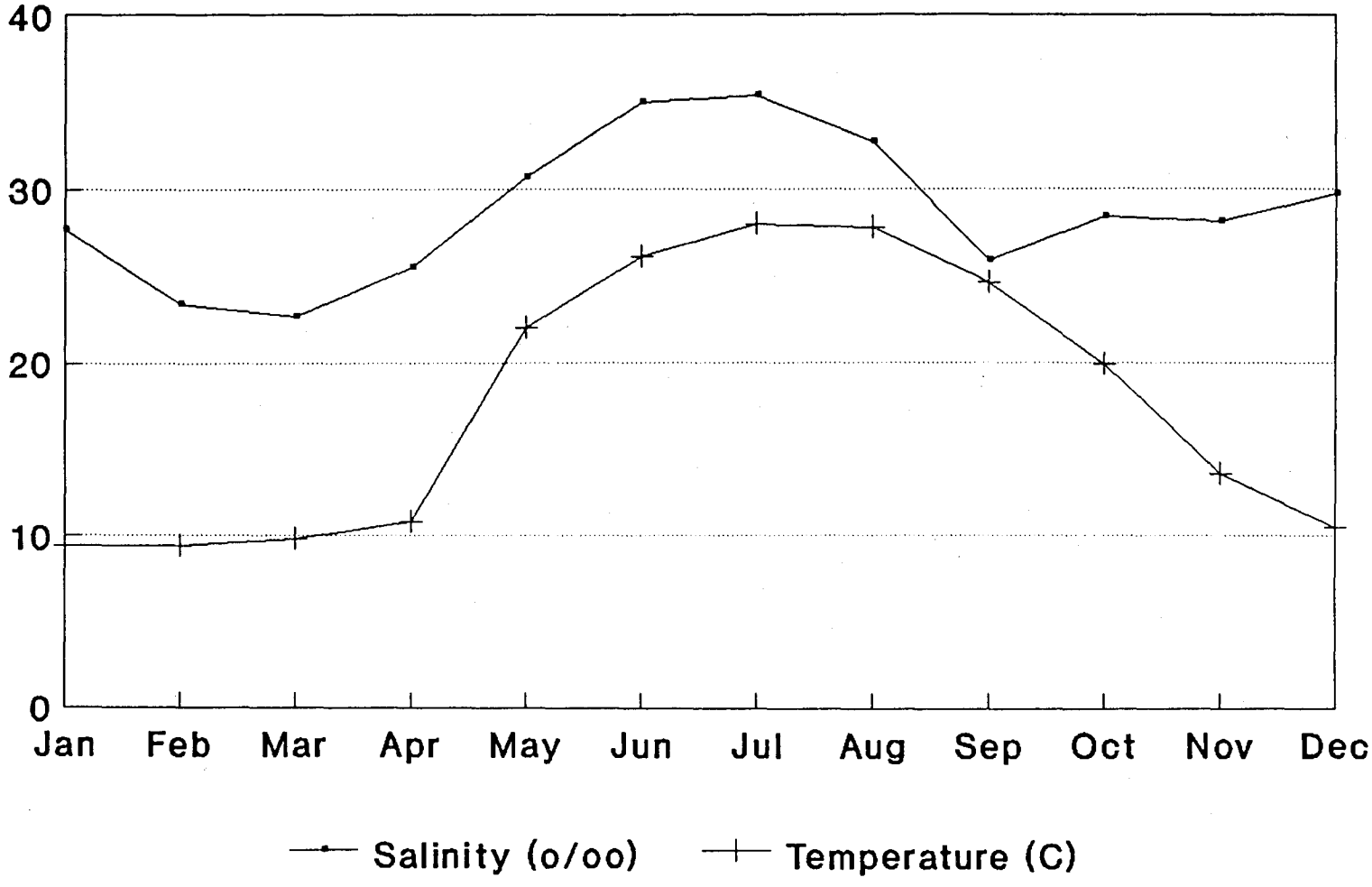
40
30
20
10
0
Jan
Feb
Mar
Apr
May
Jun
Jul
Aug
Sep
Oct
Nov
Dec
Salinity (o/oo)
Temperature (C)

APPENDIX I

Roth ('84) recommended two fixatives for immunolabelling: glutaraldehyde (4-0.5%) and a mixture of paraformaldehyde (4-2%) and glutaraldehyde (2-0.1%). Although osmium tetroxide routinely is used for TEM preparations as a post fixative, it can not be tolerated by many antigens (Roth, '84), and therefore was not used in this study.

Glutaraldehyde provides good ultrastructural preservation, however, it has several disadvantages. It inhibits tissue antigenicity, permits the loss of cellular material, such as proteins, and forms irreversible crosslinks with the amino groups of lysine. (Roth, '84) Since hydroxylysine is a major component of 140 CP, glutaraldehyde was not the optimal fixative for this study. The second fixative, a paraformaldehyde/glutaraldehyde mixture, minimized the disadvantages of glutaraldehyde but maximized the preservation of the ultrastructural integrity. Paraformaldehyde is not recommended for ultrastructural preservation except when mixed with small amounts of glutaraldehyde. The reaction between paraformaldehyde and proteins also results in crosslinks, but these are reversible in water. (Hayat, '81)

Noticeable differences were seen between tissues prepared with glutaraldehyde and the paraformaldehyde/glutaraldehyde mixture. Specimens fixed

with glutaraldehyde yielded a lower affinity for the gold label. This observation agrees with the literature. For this reason all results were from tissue prepared with the paraformaldehyde/glutaraldehyde mixture. The poor resolution and ultrastructural preservation expected from the paraformaldehyde prepared tissue was not observed.

APPENDIX II

Two embedding resins were employed. According to Causton ('84) EMBed 812 allows high resolution and good beam stability (ie. reduced section burning). Its high hydroxy content, however, facilitates hydrogen bonding and inhibits antibody diffusion. EMBed 812 also consists of many hydrophobic groups which promote non-specific labelling. L.R. White, a polyhydroxy aromatic acrylic resin, has two advantages: 1) hydrophilic groups are built into it which minimizes non-specific binding and 2) the crosslink density of the acrylic minimizes interference with antibody penetration while maximizing electron beam stability. The negative aspect of L.R. White is reduced resolution. (Causton, '84)

In this study, no difference was observed between the two resins in labelling capabilities. A difference was seen in the resolving power with L.R. White typically furnishing the better picture with minimal staining. This finding was surprising, in that with most tissues, EMBed 812 generally yields a better image. With L.R. White, one second staining in 8% uranyl acetate was sufficient where as the EMBed 812 required a staining time of 10 minutes. The shorter staining time was preferred since long exposure of the heavy metal uranium can displace the gold markers. In the final analysis labelling differences were minimal and both EMBed 812 and L.R. White sections were used.

APPENDIX III

Isolation of Insoluble Matrix Fraction

The tissues of the colonies that contain the spicules were stripped from their axes, weighed, and washed with 0.02 M NH_4HCO_3. The tissue was suspended in 10 volumes of 0.25 M NaCl in 0.2 M NH_4HCO_3 buffer adjusted to pH 8.0 The spicules remained insoluble under these conditions. They were released from their surrounding tissues by digestion (24 h, at 37C, with shaking) with 1% papain (substrate/enzyme, w/w) activated with 0.005 M cysteine. The tissues surrounding the spicules were completely digested following this treatment. The remaining spicules were washed thoroughly with the above buffer and retained on a 250 um mesh sieve. The spicules were contained in the sieve and washed thoroughly with the same buffer to avoid any possible contamination by enzyme or solubilized material.

Spicules were suspended in an equal volume of 0.5 M potassium EDTA in 0.05 M NH_4HCO_3, pH 8.0, and demineralized. The total content was recovered from dialysis tubing and centrifuged. The insoluble organic matrix residue was washed 3 times with 0.2 M NH_4HCO_3, 6 times with 0.05M NH_4HCO_3, and 3 times with distilled water. The washed insoluble matrix was lyophilized. (Kingsley et al., '90)

Production of Primary Antibody

After treatment with chitinase to remove carbohydrate moieties, the insoluble matrix was partially solubilized in

n-butanol, followed by homogenization with 8 M guanidine-HCl containing 10 % B-mercaptoethanol and 0.1 M Tris-HCl, pH. 7.5 This completely solubilized the insoluble matrix. The homogenate was dialyzed against 5 M urea-1 M thiourea mixture containing 0.17 % B-mercaptoethanol and was fractioned by 5 to 12 % SDS-Page following the method of Laemmli and Favre (1973).

Polyclonal antibodies directed against the 140 kD collagenous proteins (insoluble), were raised in male New Zealand white rabbits. The antigens were prepared by SDS-Page. (Watabe et al., '91)

VITA

Jeffrey L. Dupree was born May 28, 1965 in Harrisonburg, Virginia. After receiving a B.S. degree in biology from Wake Forest University in 1987, he worked as a research technician at Eastern Virginia Medical School. In 1989 he entered the Graduate School of the University of Richmond where he expects to receive his M.S. degree in September, 1991. He will continue his education at the Medical College of Virginia by pursuing a Ph.D. in Anatomy.